

Effective Synthesis and Biological Evaluation of Dicoumarols: Preparation, Characterization, and Docking Studies

Aziza Mnasri,* Nasser Amri, Houcine Ghalla, Rafik Gatri, and Naceur Hamdi*

Cite This: *ACS Omega* 2023, 8, 14926–14943

Read Online

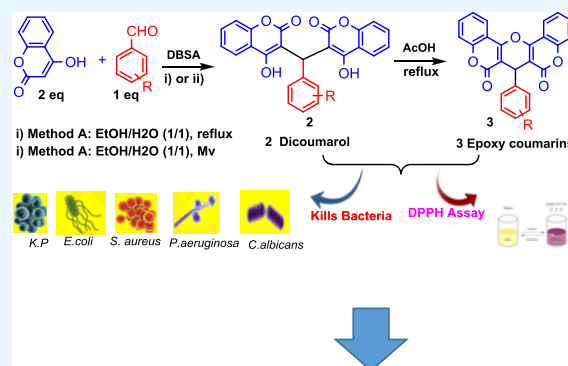
ACCESS |

Metrics & More

Article Recommendations

Supporting Information

ABSTRACT: A series of 3,3'-arylidene bis (4-hydroxycoumarins) **2** were synthesized by the reaction of aromatic aldehydes with 4-hydroxycoumarin using dodecylbenzenesulfonic acid as Brønsted acid-surfactant catalyst in aqueous media and under microwave irradiation. The present method is operationally simple and the use of water as the reaction medium makes the process environmentally benign. The epoxydicoumarins **5** were then obtained with a good yield by heating 3,3'-arylidenebis-4-hydroxycoumarins **2** in acetic anhydride. Techniques such as elemental analysis, ^1H , ^{13}C - ^1H NMR, and infrared spectroscopy were employed to characterize these compounds. The synthesized compounds displayed good antibacterial potential against *Escherichia coli* (ATCC 25988), *Pseudomonas aeruginosa* (ATCC 27853), *Klebsilla pneumonia* (ATCC 700603), *Staphylococcus aureus* (ATCC 29213), methicillin-resistant *Staphylococcus aureus* (ATCC 43300) and *Candida albicans* (ATCC 14053). The MIC values of 23 mg/mL for compound **5e** against *Escherichia coli* (ATCC 25988) and 17 mg/mL for **2a** were observed. Furthermore, a molecular docking simulation has been performed to evaluate the antibacterial activities and the probable binding modes of the studied compounds **2a–f** and **5a–g** toward the active sites of a series of well known antibacterial targets. Among the investigated compounds, the binding modes and docking scores demonstrate that **2a** has the most antibacterial and antifungal activities. Additionally, DPPH (2,2-diphenyl-1-picrylhydrazyl) and ABTS has been tested for their ability to scavenge hydrogen peroxide and free radicals. According to our results, these compounds exhibit excellent radical scavenging properties. Furthermore, compounds **2–5** were evaluated for anti-inflammatory activity by indirect haemolytic and lipoxygenase inhibition assays and revealed good activity.



1. INTRODUCTION

There has been an increase in interest in the chemistry of oxygenated heterocycles,¹ coumarins are benzo-fused heterocycles containing oxygen atom and their synthesis is important because of their widespread occurrence in nature.^{2,3} Warfarin and dicoumarol (3,3'-methylenebis [4-hydroxy-2H-1-benzopyran-2-one]^{4,5} were just a few examples of biological and pharmacological products that contained coumarin derivatives. Dicoumarol has been thoroughly explored as a natural anticoagulant medication^{6,7} due to its use in the pharmaceutical study. Dicoumarols are obtained through a straightforward condensation reaction between 4-hydroxycoumarin and aldehydes using various catalysts and media. There are numerous reported methods for synthesizing these compounds, including the use of catalysts like sodium dodecyl sulfate, ionic liquids with Lewis acid/Bronsted acid sites, molecular iodine, $\text{Ce}_2(\text{SO}_4)_4\cdot\text{H}_2\text{O}$, *p*-dodecyl benzenesulfonic acid/piperidine, SO_3H functionalized ionic liquids, sulfated titania, and nano-silica catalysts.^{8–16} Numerous synthetic techniques utilizing 4-hydroxycoumarin have recently been developed for the synthesis of biscoumarins in aqueous conditions, in response to the growing public concern about

the environment. Despite their effectiveness and environmental friendliness, these techniques require catalysts, such as TEBA¹⁷ and I_2 ,¹⁸ and have long reaction times. Therefore, innovative and effective techniques built on a green methodology are still needed. Thus, it is still required to propose efficient and novel methods based on green methodology. *p*-Dodecylbenzenesulfonic acid (DBSA) is a Brønsted acid surfactant-combined catalyst, which is composed of an acidic group and a hydrophobic moiety. It might be argued that this occurs because the interior of emulsion droplets composed of substrate and DBSA is sufficiently hydrophobic to keep water molecules out. As a result, one of the most difficult research problems has emerged in the area of surfactant-catalyzed organic processes in water. In the synthesis of bis(indol-3-yl) alkanes, tetrahydrobenzo[*b*]pyrans, dihydropyrano[*c*]-

Received: October 21, 2022

Accepted: March 22, 2023

Published: April 17, 2023



Scheme 1. Protocol Synthesis of Dicoumarol Derivatives 2

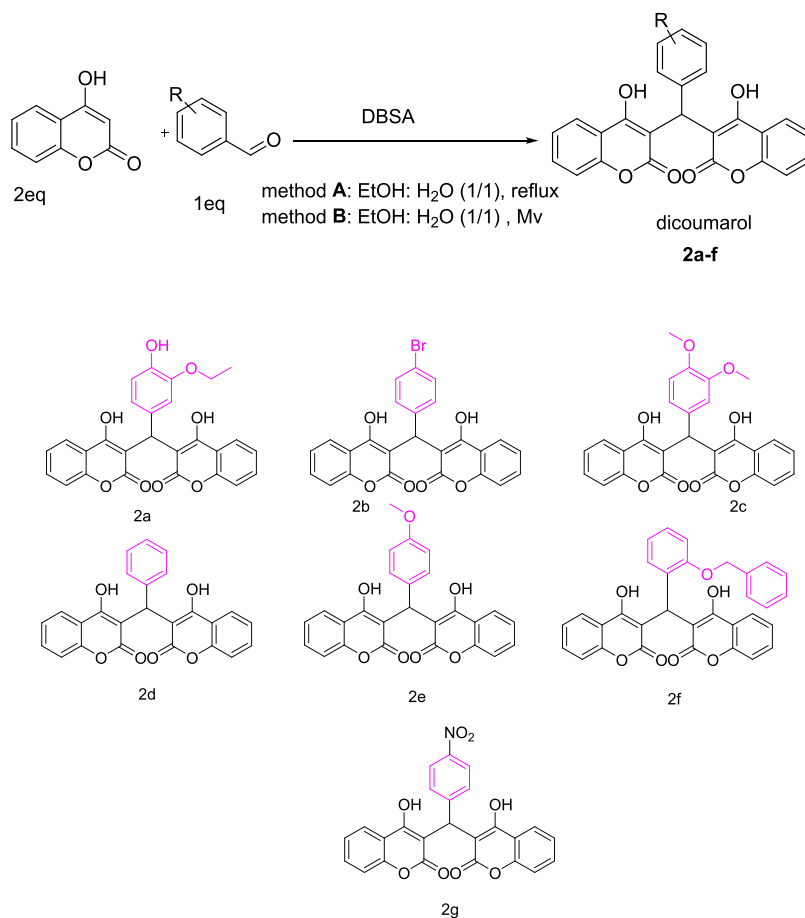


Table 1. Optimization of Reaction Condition on the Yield of 3,3-Arylidene Bis(4-hydroxycoumarin)

entry	catalyst	solvent	temperature	time/(min)	yield/% ^a
1	without DBSO	H ₂ O	reflux	240	trace
2	DBSO (25%)	H ₂ O	reflux	75	85
3	DBSO (25%)	EtOH	r.t.	120	trace
4	DBSO (25%)	EtOH	reflux	60	87
5	DBSO (25%)	MeOH	reflux	105	80
6	DBSO (25%)	EtOH/H ₂ O (1/1)	reflux	40	94
7	DBSO (25%)	EtOH/H ₂ O (1/1)	reflux	65	90
8	DBSO (25%)	EtOH/H ₂ O (1/1)	reflux	40	trace
9	DBSO (25%)	EtOH/H ₂ O (1/1)	r.t.	40	68
10	DBSO (10%)	EtOH/H ₂ O (1/1)	reflux	40	70
11	DBSO (15%)	EtOH/H ₂ O (1/1)	reflux	40	72
12	DBSO (20%)	EtOH/H ₂ O (1/1)	reflux	40	93
13	DBSO (25%)	EtOH/H ₂ O (1/1)	MV condition	12	95

^aIsolated yield

chromens, xanthenes derivatives, and esterification of different carboxylic acids and alcohols, the behavior of DBSA as a catalyst has been investigated.^{19–25} In the present work, we describe here the synthesis of 3,3-arylidene bis(4-hydroxycoumarin) **2** derivatives by DBSA and their epoxy coumarins in environmentally benign conditions and under microwave irradiation. Furthermore, these compounds had antimicrobial properties, which were measured. The antioxidant properties of all these compounds were evaluated via DPPH and H₂O₂ assays. They have shown excellent antioxidant potential. In addition the anti-inflammatory activity by indirect haemolytic

and lipoxygenase inhibition assays of compounds **2–3** were studied. Molecular docking was also utilized to predict the binding mode of dicoumarols to the protein target, and MD simulation studies were further performed on the best binding scores.

2. RESULTS AND DISCUSSION

In this study, two efficient methods for the condensation of aldehydes with 4-hydroxycoumarin were presented. These methods gave the corresponding 3,3-arylidene bis(4-hydrox-

ycoumarin) **2** in the presence of DBSA as a homogeneous catalyst (**A**, **B**) (Scheme 1).

In order to catalyze this reaction, DBSA was utilized as a source of H⁺ and was successful in preparing 3,3-arylidene bis(4-hydroxycoumarin) **2**. For the model reaction 3-nitro benzaldehyde with 4-hydroxycoumarin in the presence of DBSA in water at reflux, the systematic assessment of several solvents was initially the main focus. Attempts were made to study and optimize the reaction conditions in order to show that performing the reaction in H₂O with low yield while using the amounts of EtOH in the media produced satisfactory results (Table 1, entry 6). These results revealed that the highest yield was obtained with the water/ethanol (1:1) solvent system (Table 1, entry 6).

Since DBSA was emerged as a suitable catalyst for the reaction in 1:1 ethanol/water media, efforts were then made to optimize the catalyst load for the condensation reaction, leading to the rapid formation of 3,3-arylidene bis(4-hydroxycoumarin) **2**. According to the current optimization experiments, the yield increased steadily with catalyst load up to 25 mol %, and using more catalyst did not boost the yields; on the contrary, using less catalyst resulted in lower yields. Without a catalyst, a very small amount of the product was generated. To find the specific effect of microwave irradiation on the reaction, these reactions were carried out under the same conditions in a microwave oven (Table 1, entry 13) and it was observed that, while the reaction time considerably decreased, the yields of the product slightly increased even though the reaction time significantly lowered. Therefore, MW conditions were advantageous for this reaction. Then, to test the viability of this approach, the synthesis of a library of 3,3-arylidene bis(4-hydroxycoumarin) derivatives using two ways was studied and the obtained results are summarized in Table 2.

Table 2. Synthesis of 3,3-Arylidene Bis(4-hydroxycoumarin) by Condensation of Aldehydes and 4-Hydroxycoumarin Using DBSA (25 Mol %) as Catalyst^a

entry	Ar	method A time (min)/ yield (%)	method B time (min)/ yield (%)
2a	3-ethoxy-4-hydroxy-C ₆ H ₃	60/80	6.5/84
2b	2-Br-C ₆ H ₄	45/90	7.5/80
2c	3,4-dimethoxy-C ₆ H ₃	60/90	4.5/90
2d	-C ₆ H ₅	60/87	7/92
2e	4-methoxy-C ₆ H ₄	60/85	5.5/76
2f	2-benzyloxy-C ₆ H ₄	90/88	8/85
2g	4-NO ₂ -C ₆ H ₄	45/90	6/93
		90/85	8.5/88

^aMethod A: EtOH:H₂O (1:1), reflux; Method B: EtOH:H₂O (1:1), MV.

A variety of dicoumarols **2** were obtained utilizing various aldehydes and 4-hydroxycoumarin in the standardized process, as shown in Table 2. The compounds were obtained in high to excellent yields regardless of the kind of substitution (electron donating and electron withdrawing) of the aromatic aldehydes (entries 1–17). Similar outcomes in the microwave condition were also attained (method B). In methods A and B, all of the reactions were finished within 45 to 150 min and 4.5 to 15 min, respectively. The purification of the products using a column was not necessary in these reactions. Simply removing

the solid products from the reaction mixture, dissolving them in hot ethanol, refiltering to remove any catalyst contamination from the product, and then recrystallizing the filtrate to produce the pure dicoumarols **2** were the steps taken to obtain these products. The formation of 3,3-arylidene bis(4-hydroxycoumarin) **2** could be explained by the Knoevenagel condensation of aromatic aldehydes with 4-hydroxycoumarin in the presence of DBSA, followed by the Michael addition of the second 4-hydroxycoumarin. (Scheme 2).

Scheme 2 displays a plausible reaction mechanism. First, condensation between 4-hydroxycoumarin and the aryl benzaldehyde results in the formation of intermediate *i*₁. The compound **2** is produced when 4-hydroxycoumarin molecule attack *i*₁ through a Michael-type addition and *i*₂ is then enolized to give the final product **2**.

The condensation reaction between aromatic aldehyde and 4-hydroxycoumarin employing DBSA as a homogeneous catalyst in aqueous media under microwave conditions afford dicoumarols **2**. These conditions had benefits like a quicker reaction time, an easier setup, cheap and non-toxic catalysis, environmental friendliness, and high yields. Studies on the mass spectrum, IR, ¹H, and ¹³C NMR properties of these compounds were performed.

According to ¹H NMR, the Michael addition reaction was followed by all of the dicoumarol compounds. 3-Ethoxy-4-hydroxybenzaldehyde, 4-bromobenzaldehyde, 3,4-dimethoxybenzaldehyde, benzaldehyde, 4-methoxybenzaldehyde, 2-benzyloxybenzaldehyde, and 4-nitrobenzaldehyde all condensed to produce dicoumarol molecules. These compounds were described using spectroscopic and analytical methods. The composition was determined by elemental studies, and MS spectrum analysis further supported this conclusion. CDCl₃ was used to conduct ¹H and ¹³C-¹H NMR tests on all the compounds. As for dicoumarols, dicoumarols' NMR assignments are based on Figure 1.

All dicoumarols **2** exhibit a singlet at 11.28–11.56 ppm in the ¹H NMR proton spectrum, which is attributed to those enolic protons.²⁶ The methylene group of the aldehydes, which joins the two moieties, was given a singlet at 8 ppm. Due to the potential tautomerism that may be noticed in this singlet can also be observed at about 9.8–12 ppm (Scheme 3).

In contrast to compounds **2a** and **2g**, which were found to vibrate at frequencies between 1639 and 1652 cm⁻¹, dicoumarol structure **A** (shown in Scheme 4) was ascribed to compounds **2d**, **2e**, and **2g**. Carbonyl stretching frequencies for compounds **2a** and **2g** were found to be at 1641 and 1654 cm⁻¹, respectively, which is about 20 cm⁻¹ less than for compounds **2d**, **2e**, and **2f**, and a dichromene structure (structure B) was assigned as shown in Scheme 4.

The lactone ring's C–O stretching frequency was shown to be between 1090 and 1120 cm⁻¹. The frequency of the ketone carbonyl carbon was assigned at 1040 cm⁻¹.

The band of the hydroxyl group is slightly visible in this situation because the hydroxyl group participates in hydrogen bonding.²⁷ A singlet at 11.29 ppm in the ¹H-NMR spectra of dicoumarol **2a** was recognized as the proton of the phenolic OH group.

Similar to this, the proton of the coumarin ring, H₁₀, was observed as a singlet at 10.79 ppm. The rest of the signals for compounds **2** were assigned to the protons of the aromatic ring system. The compounds were also confirmed by ¹³C-¹H NMR, which has peaks at 166.9 ppm, attributed to the ketone's

Scheme 2. Possible Mechanism for 4-Hydroxycoumarin Condensation with Aryl Aldehydes

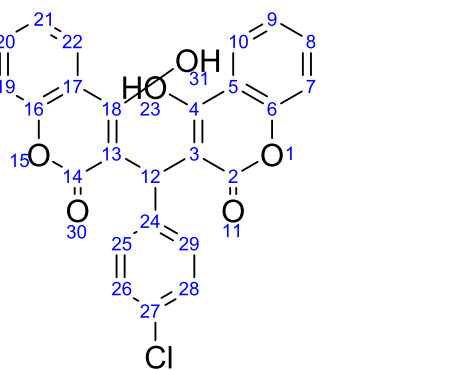
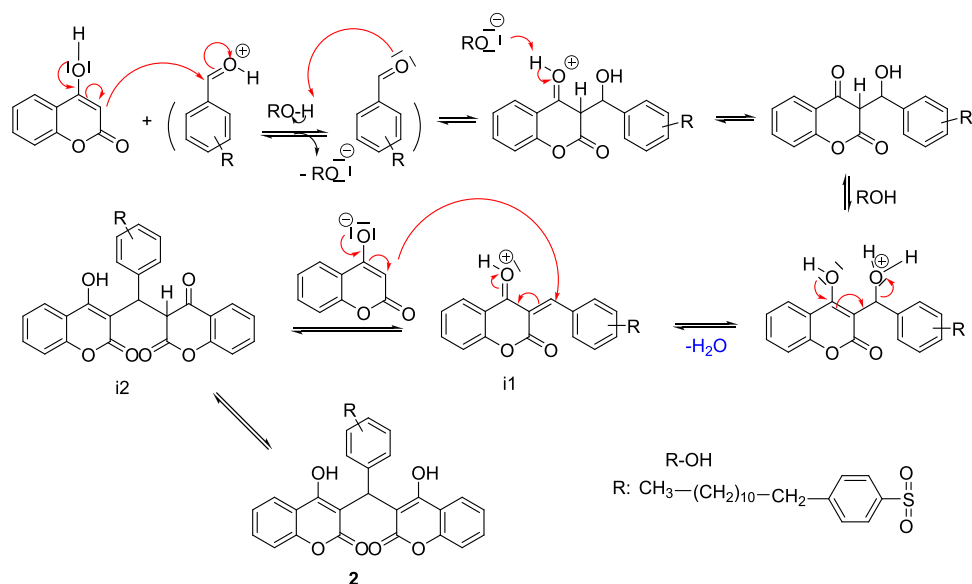
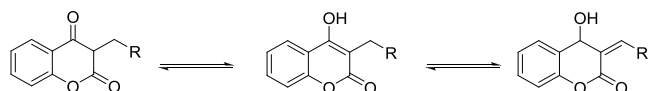


Figure 1. Atom numbering used for NMR signals for dicoumarols.

Scheme 3. Tautomerism in the Coumarin Structure



Scheme 4. Dicoumarol and Dichromone Structures



C=O group. The peak that appeared at 169.3 ppm was due to the lactone C=O.

One resonance signal is produced by the protons of the methylene groups, most likely as a result of a rapid tautomeric exchange of their chemical shifts. This suggests the dicoumarols **2** structure A (Scheme 4). The CH proton was resonated at 6 ppm depending on the aromatic aldehyde structure.^{28–30} The aromatic protons show multiplets in the region of 6–9 ppm. The ¹³C–{¹H} NMR also support the ¹H NMR spectral analyses. The presence of sp² hybridized carbon atoms of compound **2b** is shown in the ¹³C NMR spectra in

the range between 104.2 and 169.4 ppm. The lowest chemical shift was obtained for Ca (28.4 ppm). The ¹³C NMR spectrum of compounds showed also three carbon signals at δ = 36.02, 152.4, and 164.6 ppm, referring to the (C₁₂), C₂₄, and C₂₅ groups. The signals present at δ = 166.9 ppm and δ = 169.3 ppm are assigned to the C-4 carbon.

The ¹H NMR spectrum of compound **5g** was chosen as a model, and the spectral data were recorded using CDCl₃ as solvent. The ¹H NMR spectrum of **5g** in CDCl₃ shows an OH sharp singlet signal at δ = 11.43 ppm, and this signal disappeared in CDCl₃. This is likely due to the proton exchange between the residual water of solvent (CDCl₃) and compound **5g**. In CDCl₃, the aromatic protons appeared in the range of λ = 6.54–6.75 ppm and the sharp singlet signal at λ = 6.17 ppm correspond to CHC=O.

The hybrid framework of the coumarin nucleus with other moieties and the improved pharmacological property have been a topic of interest. In view of the above observations, the synthesis of some coumarin derivatives were synthesized from the condensation reaction between 4 mol equiv of 4-hydroxycoumarin and 1 mol eq of isophthalaldehyde and terephthalaldehyde (Scheme 5). This method is useful for aromatic aldehydes because the insoluble products were easily separated by filtration. The synthesized compounds have an excellent yield. FTIR spectra of these compounds show a strong absorption band around 3084–3471 cm⁻¹ assigned to the O–H stretching. In addition, the stretching vibration was observed at 1714–1745 cm⁻¹ due to a carbonyl group (C=O) of coumarin. ¹H NMR of these derivatives revealed the presence of a singlet at 9.19–8.99 ppm for –OH–. The derivatives of the coumarin ring proton (C_{coum}.H₄) were observed as a singlet at 8.98–8.20 ppm. All the other aromatics protons were observed within the expected regions. ¹³C NMR of these compounds was in concordance with the proposed structure of substituted coumarin derivatives. The two new signals at 115 and 136 ppm show carbon of coumarin (C₃ coum. and C₄ coum.), respectively.

The epoxycoumarins **5** were obtained by heating dicoumarols derivatives **2** in acetic acid anhydride (Scheme 6). The target compounds' structures **5** were verified by IR, ¹H, ¹³C,

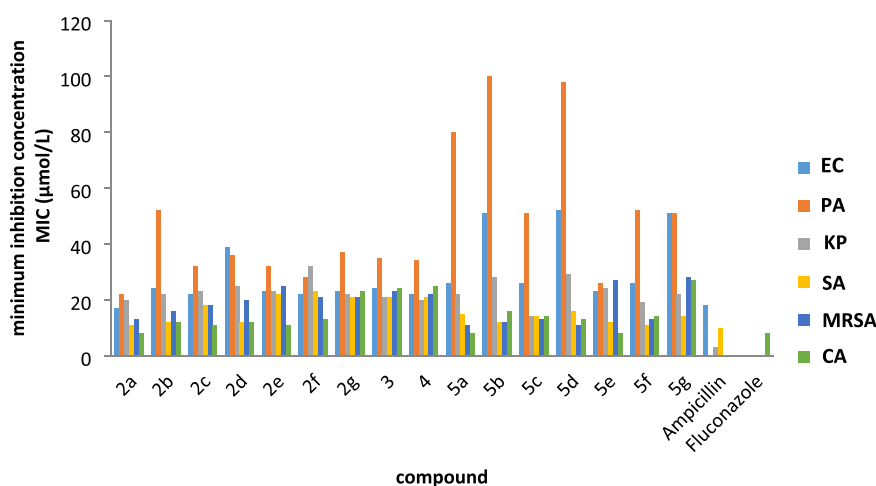


Figure 2. Minimal inhibitory concentration micro mol/L of compounds 2–5 against bacterial and fungal strains. EC: *Escherichia coli* (ATCC 25988). PA: *Pseudomonas aeruginosa* (ATCC 27853). KP: *Klebsilla pneumonia* (ATCC 700603). SA: *Staphylococcus aureus* (ATCC 29213). MRSA: methicillin-resistant *Staphylococcus aureus* (ATCC 43300). CA: *Candida albicans* (ATCC 14053).

Table 3. Docking Score S (kcal/mol) Results of Antimicrobial Activities of 2a–f and 3a–e

ligand	1JJ	1JIL	1LXC	2WFG	3JQ9	5R80	6CJF
2a	−7.51	−7.74	−7.14	−7.45	−7.06	−7.25	−7.35
2b	−7.07	−7.24	−6.32	−6.70	−6.05	−6.34	−6.69
2c	−7.12	−7.42	−6.39	−6.86	−6.79	−7.11	−7.29
2d	−6.22	−7.01	−5.72	−6.88	−6.36	−6.44	−7.12
2e	−7.08	−7.25	−5.82	−6.78	−6.45	−6.89	−6.91
2f	−7.48	−7.69	−6.95	−7.08	−6.95	−7.16	−5.85
ampicillin	−7.16	−6.73	−5.59	−6.45	−5.40	−5.58	−6.25
5a	−6.99	−7.26	−6.30	−6.67	−6.52	−7.13	−6.91
5b	−6.83	−6.51	−5.74	−6.24	−6.01	−6.62	−5.68
5c	−7.18	−6.82	−6.00	−7.38	−6.10	−7.28	−6.51
5d	−6.65	−6.22	−5.76	−5.98	−6.55	−6.59	−6.25
5e	−7.25	−6.75	−5.94	−6.75	−6.59	−6.79	−6.50
tetracycline	−7.06	−7.22	−5.37	−6.07	−5.94	−6.23	−6.09

ampicillin and flucazole were used to test the antibacterial activity of all three substances, it can be claimed that promising results were achieved. Epoxycoumarins **5a** and **5e** exhibited the same activity with fluconazole against *Candida albicans* (ATCC 14053). Finally, the dicoumarols **2** exhibited lower or equal inhibitory effect against Gram-negative bacterial strains compared with Gram-positive bacterial strains and fungal strains. These results can be attributed to the outer membrane of Gram-negative bacteria that render them more resistant against antimicrobial agents.

4. MOLECULAR DOCKING

Molecular docking is considered a very valuable technique to evaluate the biological activity of the newly synthesized compounds **2–5** as possible antibacterial drugs and design new therapies for diseases. This technique is used to predict and examine the conformations and binding interactions of a ligand in the active site of a target enzyme. The MOE 2015.10 software package is used to evaluate and analyze both the potency and mode of action of the newly synthesized compounds as antibacterial inhibitors by studying the interactions between the compounds and the amino acid residues of the binding pocket of the target enzymes and binding energies. The molecular docking calculations have been performed to evaluate the antimicrobial activities of the

synthesized compounds **2a–f** and **5a–e**. Some efficient targets have been used to investigate the antibacterial activities of the title compounds, such as 1JJ, 1JIL, 1LXC, 2WFG, 3JQ9, 5R80, and 6CJF. The scoring values are given in Table 3. One may conclude that **2a** is the most potential antibacterial compound, with scores higher than 7 kcal/mol. The findings also revealed that **2a** has stronger antibacterial properties than ampicillin and tetracycline compounds. The best poses of top-ranked score compound **2a** in the protein targets along with their 2D binding interactions are depicted in Figures 3–10. The principal ligand–target interactions are listed in Table 4. Obviously, compound **2a** is stabilized in the active sites of the antibacterial targets through hydrogen bonding and arene–H interactions with receptor residues.

5. ANTIOXIDANT ACTIVITY

The antioxidant activity of the obtained compounds **2–5** was evaluated using the DPPH (1,1-diphenyl-2-picrylhydrazyl) antiradical test and the ABTS [2,2′-azino-bis(3-ethylbenzothiazoline-6-sul phonic acid)] scavenging assay. IC₅₀ values were used to represent the obtained results (the concentration in g mL^{−1}). Figure 10 illustrates the strong scavenging activity against the radical DPPH. The IC₅₀ values of the compounds **5** were 49.07, 48.17, 49.90, 33.05, 46.80, 34.15, and 45.15 g mL^{−1} respectively. The IC₅₀ of the compounds **2a–g** and **5a–g**

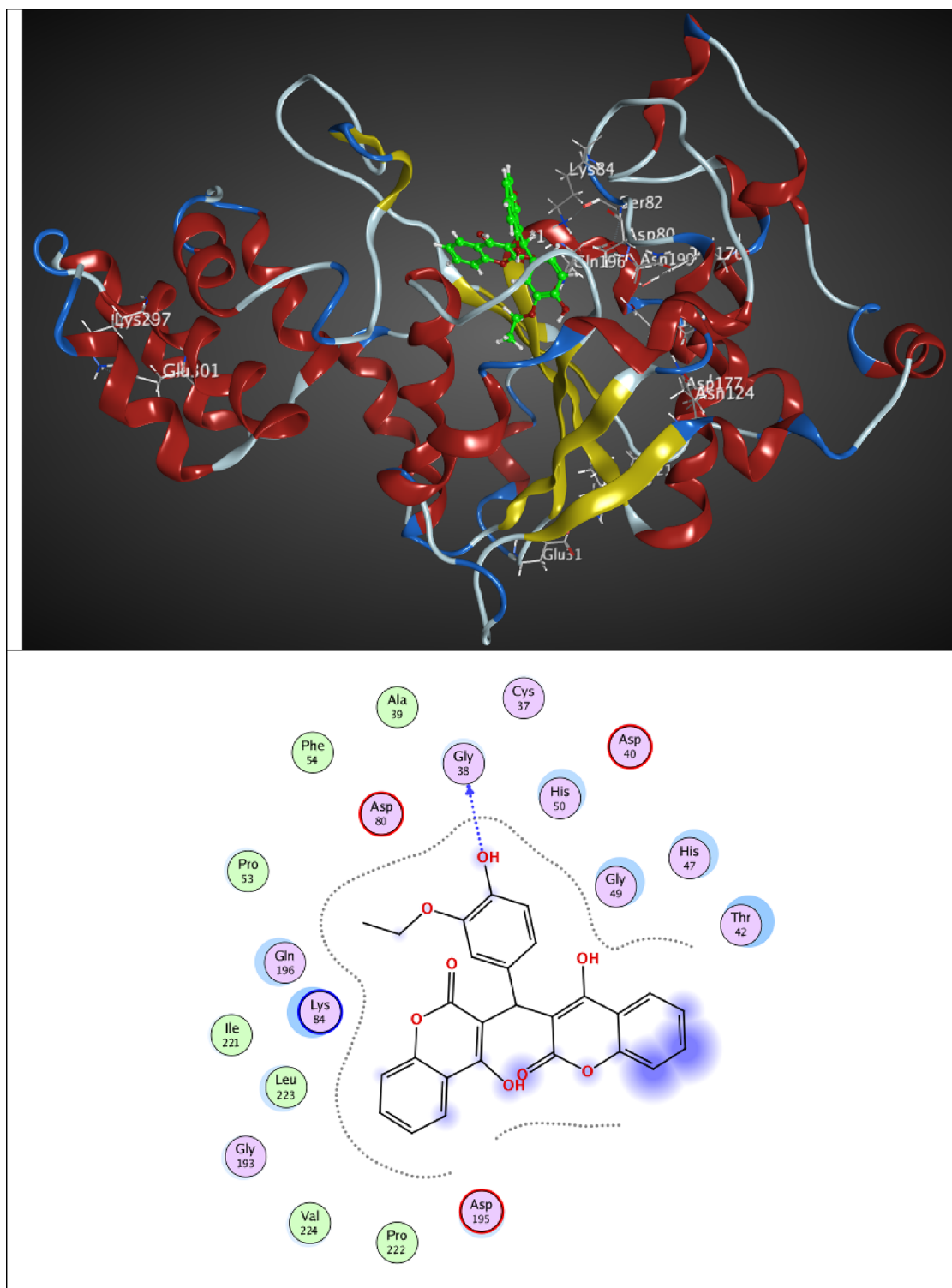


Figure 3. 3D best pose of **2a** ligand in tyrosyl-tRNA synthetase (1JII) target enzyme (top), along with 2D ligand–protein interactions (bottom).

for their activity against the free radical ABTS was highly varied and ranged between 23.04 and 34.41 g mL⁻¹. Compounds **5a** (32.22 g mL⁻¹), **5b** (31.39 g mL⁻¹), **5d** (34.17 g mL⁻¹), and **5g** (42.28 g mL⁻¹) had the highest activity in the ABTS assay (Figure 10). It should be noted that the control BHT, which is a well-known powerful antioxidant molecule, has an IC₅₀ value in the free radical ABTS of 23.38 g mL.

6. ANTI-INFLAMMATORY ACTIVITY

As per our objective, we next examined the anti-inflammatory activities of the synthesized compounds **2–5** by lipoxygenase inhibition and phospholipase A₂ (PLA₂) inhibition assays. The IC₅₀ values of the standards and test samples in both assays are given in Figure 11. In both the PLA₂ inhibition assay (26.5–34.9 M) and the lipoxygenase inhibition assay (5.0–5.1 M), the obtained compounds **2b** and **2c** showed strong anti-inflammatory efficacy. It should be noted that compounds **5b**

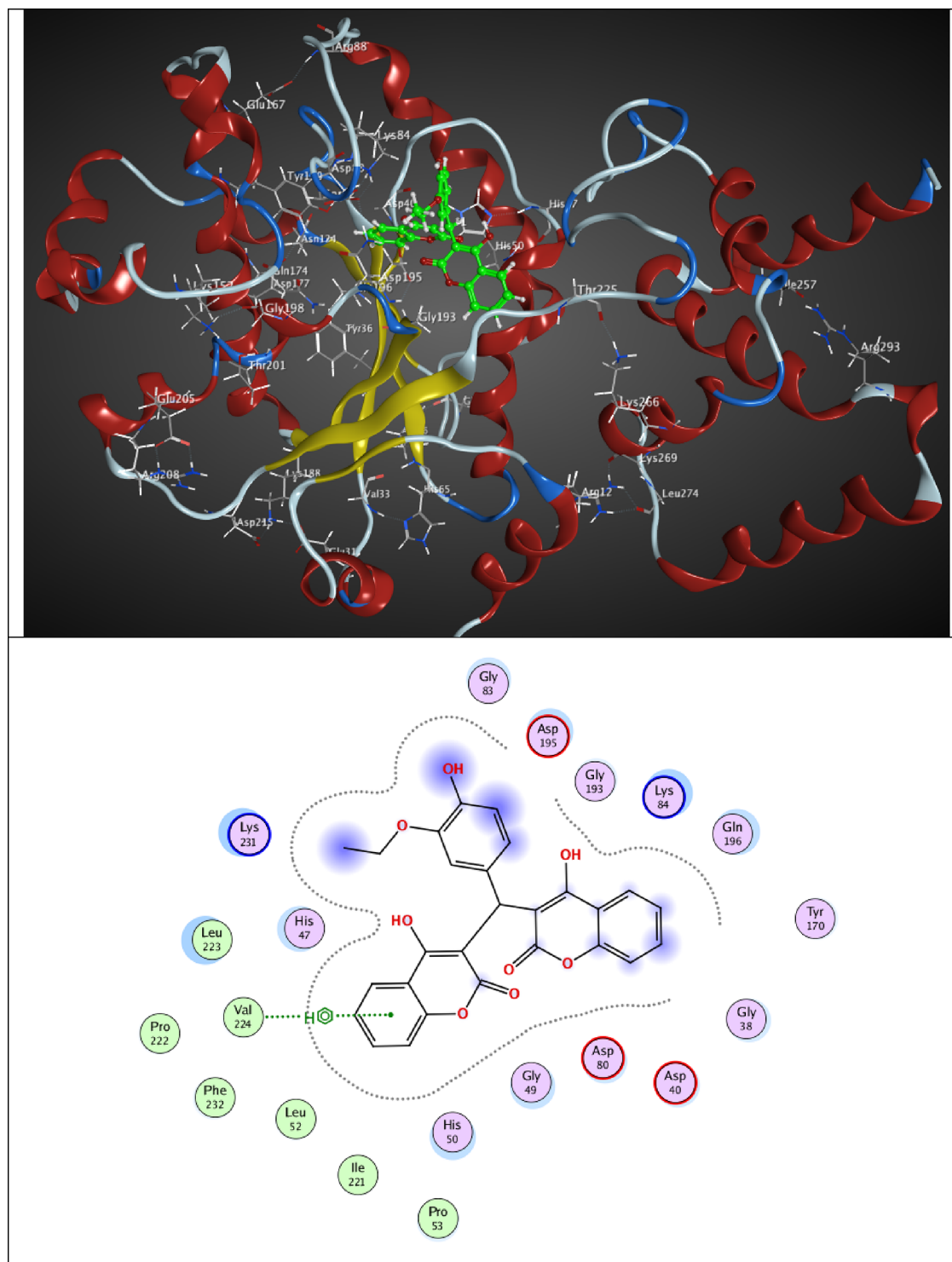


Figure 4. 3D best pose of **2a** ligand in tyrosyl-tRNA synthetase (IJIL) target enzyme (top), along with 2D ligand–protein interactions (bottom).

and **5c** almost have the same anti-inflammatory effects as industry standards indomethacin and aristolochic acid.

7. CONCLUSIONS

We describe the synthesis of new dicoumarol derivatives **2** containing ortho, meta, and para substitutions on the benzene ring and their epoxycoumarins derivatives **5**. Their antibacterial activity against *S. aureus*, *B. subtilis*, *E. coli*, and *Klebsiella sp.* and selectivity of these compounds for gram-positive bacteria were clearly demonstrated.

The utilization of dodecylbenzenesulfonic acid as a Brønsted acid-surfactant catalyst in aqueous media and under microwave irradiation should classify this chemistry as green chemistry. The obtained compounds were characterized by various spectro-analytical techniques, and it was established that dicoumarols were confirmed. The most potent antibacterial properties of compound **2a** were clearly demonstrated by molecular docking calculations using multiple targets. By using the super oxide radical, DPPH (2,2-diphenyl-1-picrylhydrazyl), and ABTS to test the anti-oxidant properties of compounds **2**–

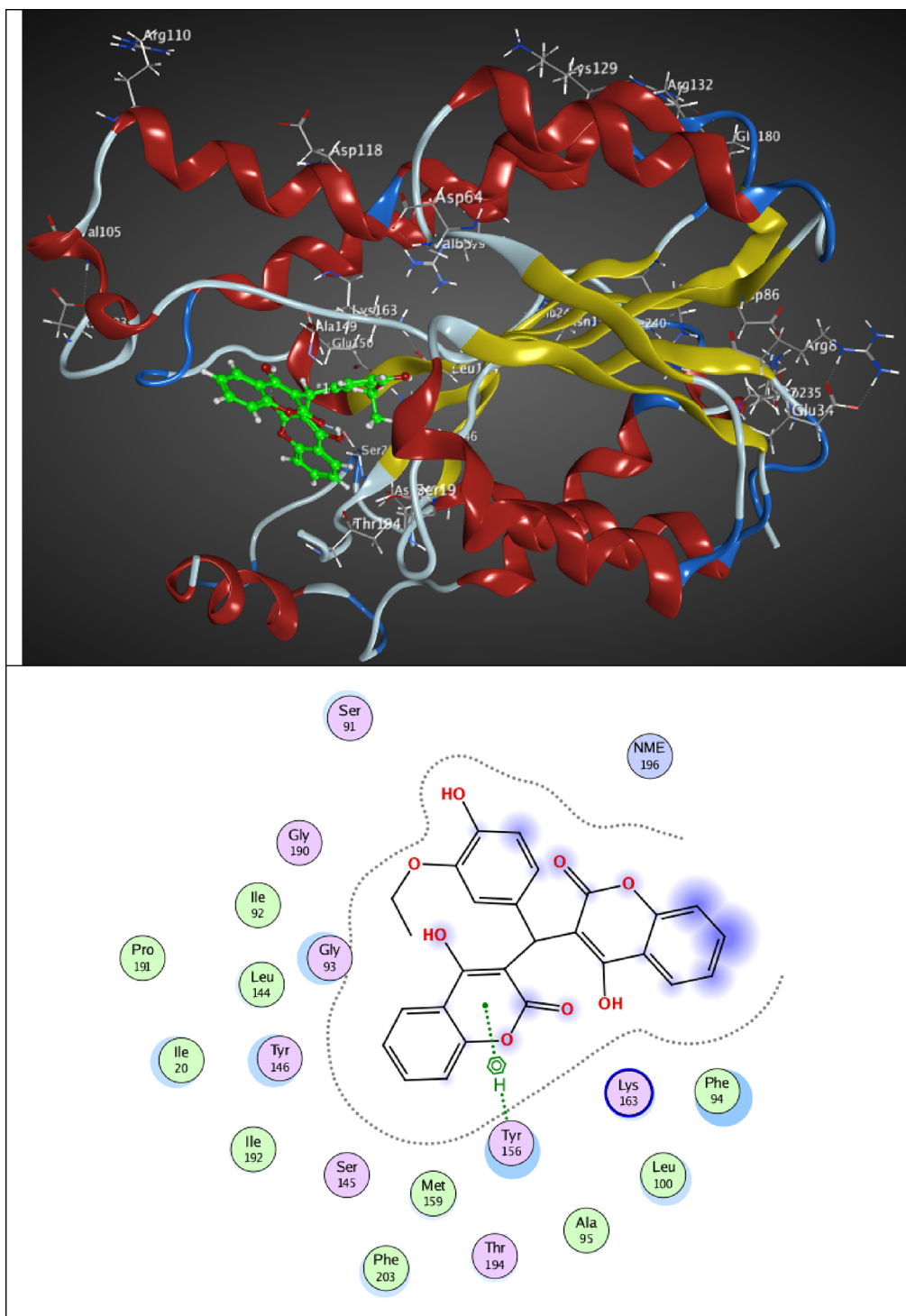


Figure 5. 3D best pose of **2a** ligand in enoyl-[acyl-carrier-protein] reductase [NADH] (1LXC) target enzyme (top), along with 2D ligand–protein interactions (bottom).

5, it was shown that the majority of them exhibited notable antioxidant properties. Furthermore, indirect haemolytic and lipoxygenase inhibition assays were used for the evaluation of anti-inflammatory activity and revealed good activity.

8. EXPERIMENTAL SECTION

8.1. Materials and Methods. All manipulations were carried out in air. All chemicals and solvents were purchased from Sigma-Aldrich and Merck. The solvents such as

dimethylformamide (DMF), dichloromethane, and diethyl ether were purified by distillation over the drying agents. Melting points were determined with an Electrothermal-9200 melting point apparatus. The elemental analysis measurements were determined by an LECO CHNS-932 elemental analyzer. Fourier transform infrared spectra were obtained in the range of 450–4000 cm^{-1} on a Perkin Elmer Spectrum 100 spectrophotometer. The mass analysis was determined by using a Thermo Scientific Exactive Plus Benchtop Full-Scan

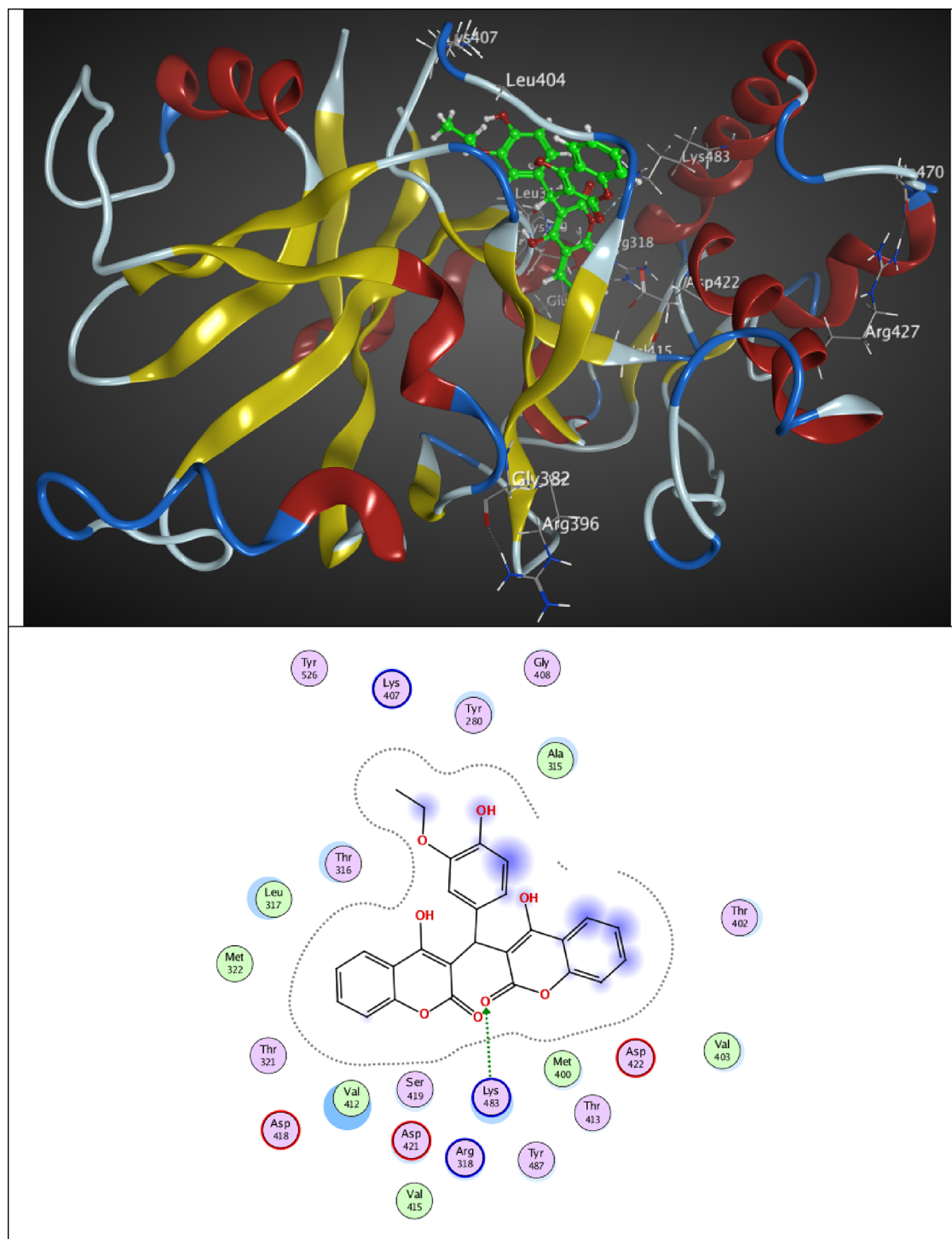


Figure 6. 3D best pose of **2a** ligand in cytosolic leucyl-tRNA synthetase (2WFG) target enzyme (top), along with 2D ligand–protein interactions (bottom).

Orbitrap mass spectrometer LC–MS/MS analyzer. ^1H NMR and ^{13}C NMR spectra were recorded at 400 (^1H) and 100 MHz (^{13}C) in CDCl_3 with tetramethylsilane as an internal reference (Malaty, Turkey). The NMR studies were carried out in high-quality 5 mm NMR tubes. Signals are quoted in parts per million as δ downfield from tetramethylsilane ($\delta = 0.00$) as an internal standard. NMR multiplicities are abbreviated as follows: s = singlet, d = doublet, t = triplet, m = multiplet. The spectroscopic data of the new compounds **2–5** are presented below.

8.2. General Procedure for the Synthesis of 3,3-Arylidene.

8.2.1. Bis(4-hydroxy-2H-chromen-2-ones) Derivatives (Method A). In 5 mL of an ethanol–water combination of 4-hydroxycoumarin (2 mmol, 0.324 g), substituted benzaldehydes (1 mmol, 0.106 g) and DBSA (0.25 mmol, 0.326 g) were mixed at reflux (1:1). The progress of the reaction was monitored by TLC. After the reaction completion and upon its cooling, the solid material was precipitated from the solution. The precipitates were filtered off, washed with water, and were recrystallized from EtOH to obtain pure 3,3-

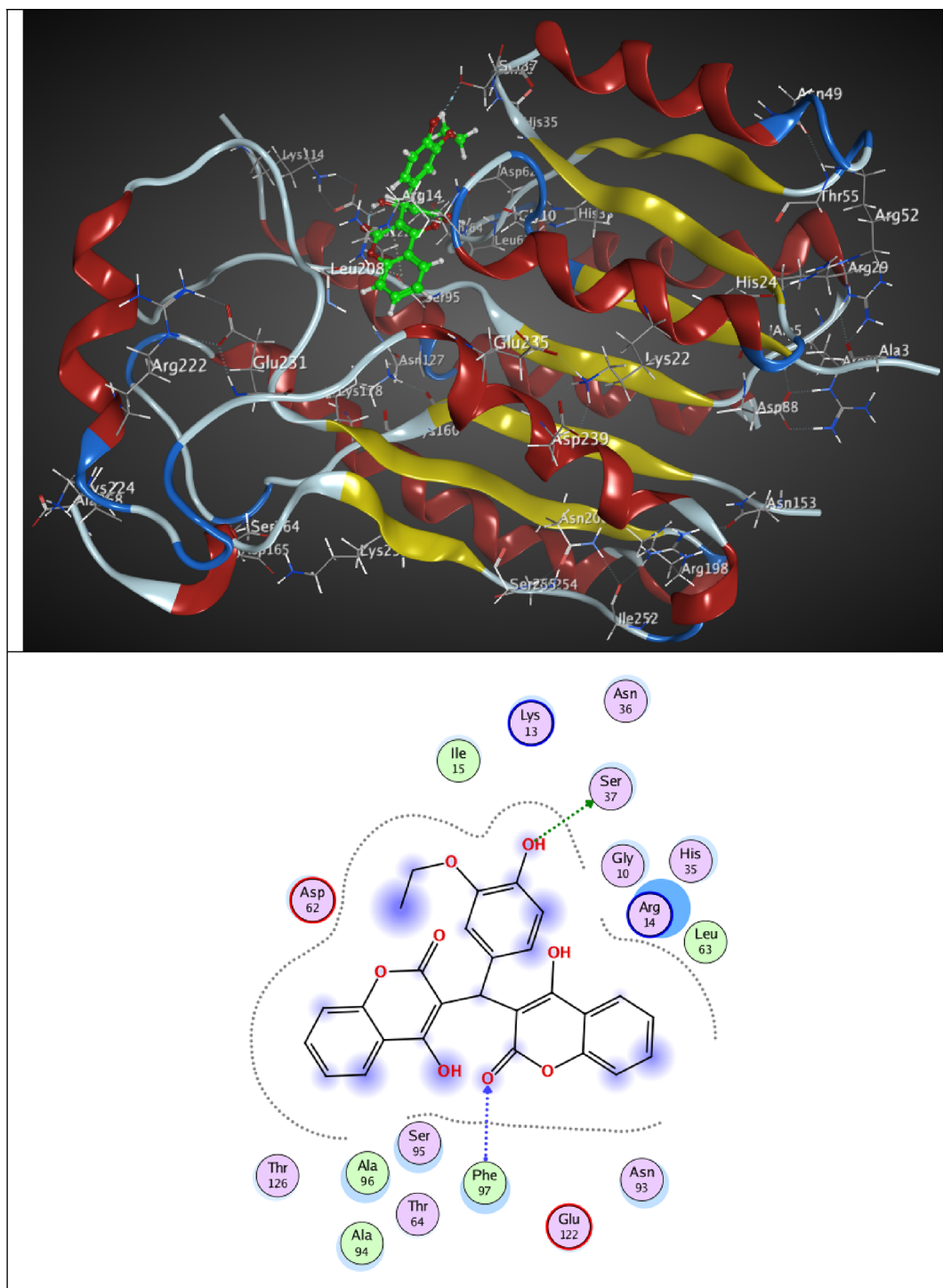


Figure 7. 3D best pose of **2a** ligand in pteridine reductase 1 (3JQ9) target enzyme (top), along with 2D ligand–protein interactions (bottom).

arylidene bis(4-hydroxy-2*H*-chromen-2-ones) derivatives as yellow-white solids (60–90% yields).

8.3. General Procedure (Method B). A mixture of substituted benzaldehydes (1 mmol, 0.106 g), 4-hydroxycoumarin (2 mmol, 0.324 g), and DBSA (0.25 mmol, 0.326 g) was placed in a microwave (Samsung, Model KE300R) at 450 W for the necessary amount of time. When the reaction was finished, the bulk was cooled to 25 °C. The solid residue was filtered off, washed with water, and were recrystallized from EtOH (68–93% yields).

8.3.1. 3,3'-((3-Ethoxy-4-hydroxyphenyl)methylene)bis(4-hydroxy-2*H*-chromen-2-one) (2a**).** Yield: 85%; m.p. 252 °C. IR ν (cm⁻¹): 3082 (OH); 1654 (CO); 1565 (C=C). ¹H NMR (400 MHz, CDCl₃) (λ , ppm): 1.24 (t, 3H, H_b); 2.65 (q, 2H, H_a); 6.1 (s, 1H, H₁₂); 7.15 (q, 4H, H_{29,28,26,25}), 7.43 (d, 4H, H_{9,21,7,19}); 7.65 (td, 2H, H_{8,20}); 8.12 (d, 2H, H_{10,22}), 11.29 (s, 1H, H₂₃); 11.52 (s, 1H, H₃₁). ¹³C NMR (100 MHz, CDCl₃) (λ , ppm): 15.55 (C_b); 28.46 (C_a); 36.02 (C₁₂); 104.17 (C_{3,13}); 105.88 (C_{5,17}); 116.75 (C_{7,19}); 124.51 (C_{10,22}); 124.96 (C_{9,21}); 126.55 (C₂₈); 128.25 (C₂₆); 132.30 (C₈); 132.91 (C₂₀); 142.92 (C₂₉); 152.45 (C₂₅); 152.65 (C₂₇); 164.64 (C₂₄); 165.79

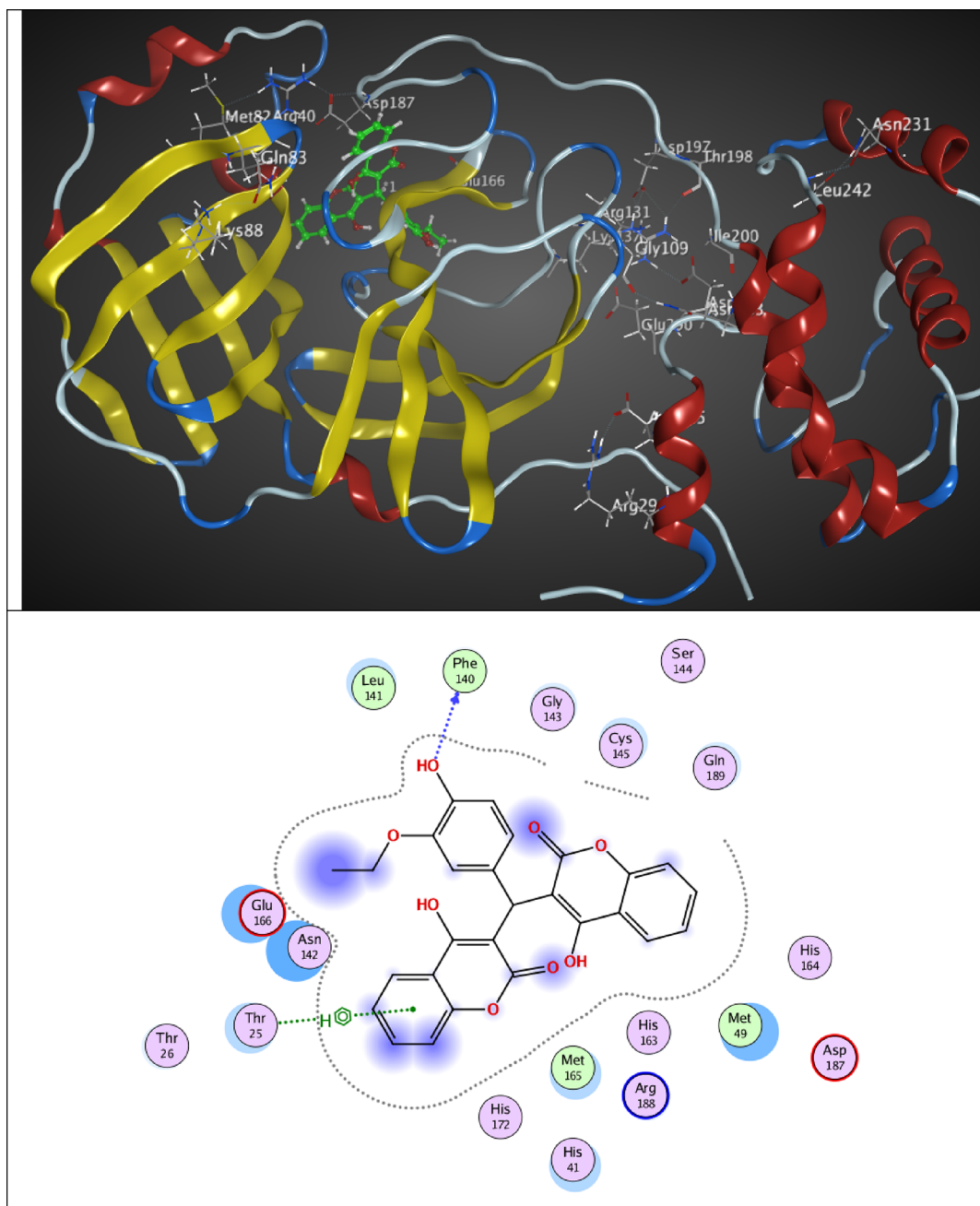


Figure 8. 3D best pose of **2a** ligand in 3C-like proteinase (5R80) target enzyme (top), along with 2D ligand–protein interactions (bottom).

(C_{6,16}); 166.97 (C_{2,14}); 169.38 (C_{4,18}). Calcd for C₂₇H₂₀O₈: C, 68.64%; H, 4.27%; O, 27.09%. Found: C, 68.7; H, 4.3; O, 6.6%.

8.3.2. 3,3'-((4-Bromophenyl)methylene)bis(4-hydroxy-2H-chromen-2-one) (2b). Yield: 86%; m.p. 245 °C. IR ν (cm⁻¹): 3065 (OH); 1667 (CO); 1607 (C=C). ¹H NMR (400 MHz, CDCl₃) (λ , ppm): 2.35 (s, 3H, H_a); 6.07 (s, 1H, H₁₂); 7.15 (q, 4H, H_{29,28,27,26}), 7.42 (d, 4H, H_{9,21,7,19}); 7.63 (td, 2H, H_{8,20}); 8.05 (d, 2H, H_{10,22}), 11.42 (d, 2H, H_{23,31}). ¹³C NMR (100 MHz, CDCl₃) (λ , ppm): 21.12 (C_a); 35.98 (C₁₂); 104.22 (C_{3,13}); 105.85 (C_{5,17}); 116.76 (C_{7,19}); 124.52 (C₂₈); 124.98 (C_{10,22}); 126.5 (C₂₉); 129.47 (C_{9,21}); 132.18 (C₂₇), 132.95 (C_{8,20}); 136.62 (C₂₆); 152.65 (C₂₄); 164.67 (C₂₅); 165.85 (C_{6,16}); 166.98 (C_{2,14}); 169.44 (C_{4,18}). Calcd for C₂₅H₁₅O₆Br: C, 61.12%; H, 3.08%; O, 19.54%. Found: C, 61.2; H, 3.1; O, 19.6%.

8.3.3. 3,3'-((3,4-Dimethoxyphenyl)methylene)bis(4-hydroxy-2H-chromen-2-one) (2c). Yield: 94%; m.p. 256 °C. IR ν (cm⁻¹): 3067 (OH); 1662 (CO); 1558 (C=C). ¹H NMR (400 MHz, CDCl₃) (λ , ppm): 6.01 (s, 1H, H₁₂); 7.15 (dd, 2H, H_{29,25}), 7.26–7.29 (m, 2H, H_{28,26}); 7.42 (d, 4H, H_{9,21,7,19}); 7.65 (td, 2H, H_{8,20}), 8.04 (dd, 2H, H_{10,22}), 11.35 (s, 1H, H₂₃), 11.55 (s, 1H, H₃₁). ¹³C NMR (100 MHz, CDCl₃) (λ , ppm): 35.95 (C₁₂); 103.85 (C₃); 105.39 (C₁₃); 116.48 (C₅); 116.82 (C₁₇); 116.96 (C_{7,19}); 124.55 (C_{10,22}); 125.14 (C_{9,21}); 128.12 (C₈), 128.91 (C₂₀); 132.86 (C_{28,26}); 133.16 (C₂₉); 133.97 (C₂₅); 152.44 (C₂₇); 152.67 (C₂₄); 164.73 (C_{6,16}), 166.15 (C₂); 166.97 (C₁₄); 169.34 (C_{4,18}). Calcd for C₂₇H₂₀O₈: C, 68.64%; H, 4.27%; O, 27.09%. Found: C, 68.7; H, 4.3; O, 27.1%.

8.3.4. 3,3'-((Phenylmethylene)bis(4-hydroxy-2H-chromen-2-one) (2d). Yield: 76%; m.p. 226 °C. IR ν (cm⁻¹): 3075

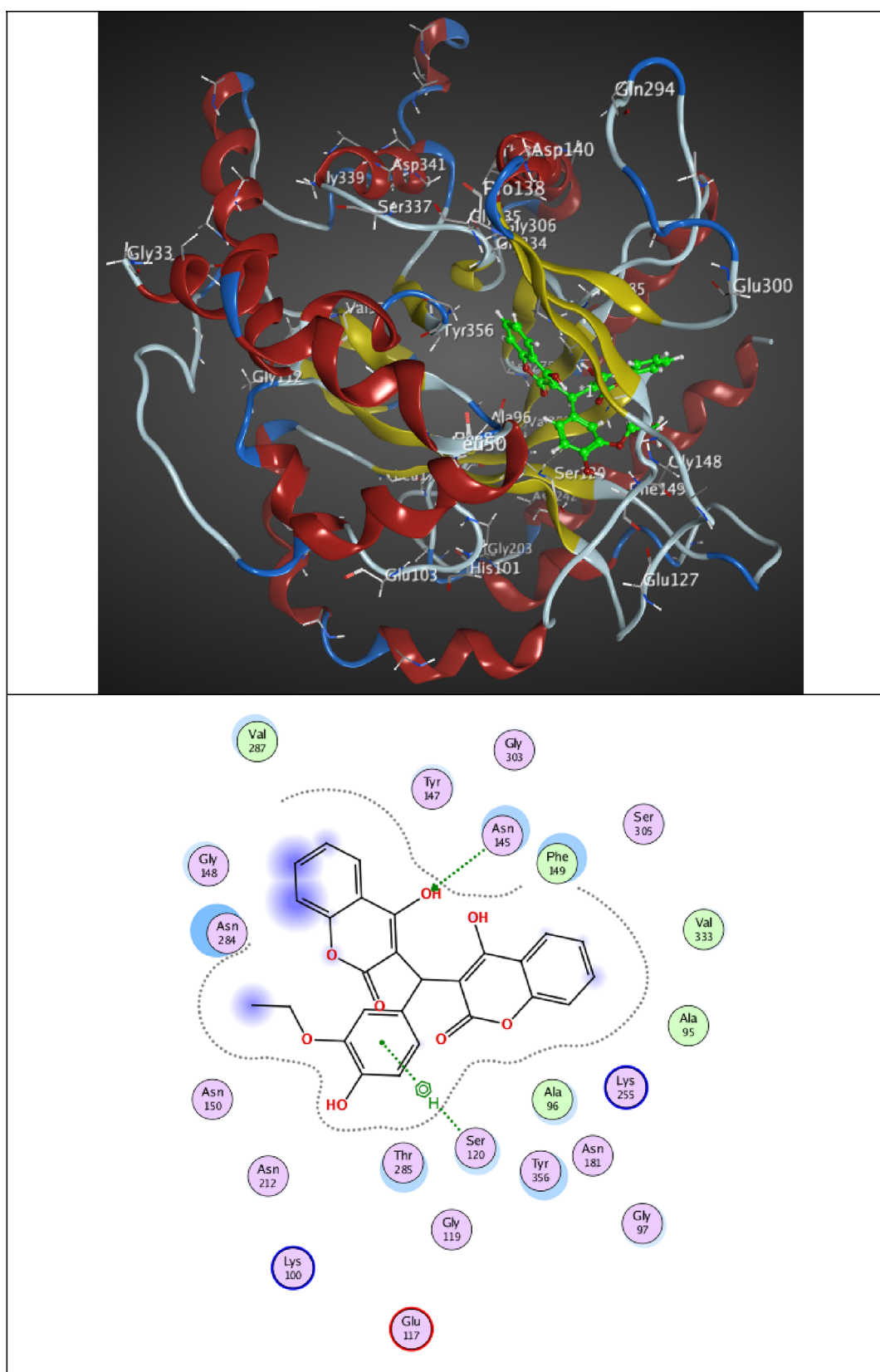


Figure 9. 3D best pose of 2a ligand in dihydroorotate dehydrogenase (quinone), mitochondrial (6CJF) target enzyme (top), along with 2D ligand–protein interactions (bottom).

(OH); 1680 (CO); 1545 (C=C). ^1H NMR (400 MHz, CDCl_3) (λ , ppm): 3.54 (s, 3H, H_d); 3.69 (s, 3H, H_b); 6.15 (s, 1H, H_{12}); 6.32–6.39 (m, 2H, $\text{H}_{29,28,27,26}$), 7.12 (dd, 1H,

$\text{H}_{9,21,7,19}$); 7.19–7.84 (m, 4H, $\text{H}_{8,20}$); 7.46 (td, 2H, $\text{H}_{10,22}$), 7.82 (dd, 2H, $\text{H}_{23,31}$). ^{13}C NMR (100 MHz, CDCl_3) (λ , ppm): 32.34 (C_{12}); 54.97 (C_d); 55.46 (C_b); 98.54 (C_{26}); 103.47

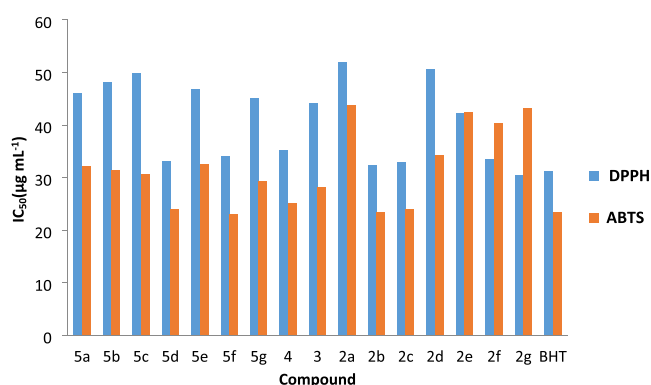


Figure 10. The antioxidative activity of compounds 2–5 synthesized was assessed by the DPPH technique and expressed as IC_{50} in $g\ mL^{-1}$. BHT was used as a control.

Table 4. 2D Ligand–Protein Interactions between 2a and Protein Targets

targets	S (kcal/mol)	interactions
1JJJ	−7.51	H-bonding O–H...Gly38
1JIL	−7.74	arene–H...Val224
1LXC	−7.14	arene–H...Tyr156
2WFG	−7.45	H-bonding C=O...Lys483
3JQ9	−7.06	H-bonding C=O...Phe97 H-bonding O–H...Ser37
5R80	−7.25	H-bonding O–H...Phe140 arene–H...Thr25
6CJF	−7.35	H-bonding O–H...Asn145 arene–H...Ser120

($C_{3,13}$); 103.94 (C_{28}); 115.32 (C_{24}); 120.25 ($C_{5,17}$); 122.71 ($C_{7,19}$); 123.29 (C_{10}), 123.95 (C_{22}); 129.25 ($C_{9,21}$); 130.46 ($C_{8,20}$); 152.35 (C_{29}); 157.95 (C_6); 158.35 (C_{16}); 164.19 ($C_{2,14}$); 167.25 ($C_{4,18}$). Calcd for $C_{25}H_{16}O_6$: C, 72.81%; H, 3.91%; O, 23.28%. Found: C, 72.9; H, 3.9; O, 23.3%.

8.3.5. 3,3'-((4-Methoxyphenyl)methylene)bis(4-hydroxy-2H-chromen-2-one) (**2e**). Yield: 95%; m.p. 227 °C. IR ν (cm^{-1}): 3072 (OH); 1665 (CO); 1545 (C=C). 1H NMR (400 MHz, $CDCl_3$) (λ , ppm): 6.22 (s, 1H, H_{12}); 7.31 (t, 6H, $H_{9,21,7,19,29,25}$), 7.65 (t, 2H, $H_{8,20}$); 8.02 (d, 1H, H_{10}); 8.03 (d, 1H, H_{22}), 8.29 (d, 2H, $H_{28,26}$), 11.39 (s, 1H, H_{23}), 11.58 (s, 1H,

H_{31}). ^{13}C NMR (100 MHz, $CDCl_3$) (λ , ppm): 36.65 (C_{12}); 103.35 ($C_{3,13}$); 104.85 ($C_{5,17}$); 116.35 (C_7); 116.75 (C_{19}); 116.85 (C_{10}); 116.93 (C_{22}); 123.95 ($C_{28,26}$); 124.58 (C_9), 124.62 (C_{21}); 125.28 (C_{13}); 125.35 (C_{25}); 127.68 (C_8); 133.45 (C_{20}); 143.48 (C_{27}), 146.95 (C_{24}), 152.45 (C_6); 152.65 (C_{16}); 164.95 (C_2); 166.56 (C_{14}); 167.28 (C_4); 169.28 (C_{18}). Calcd for $C_{26}H_{18}O_7$: C, 70.58%; H, 4.10%; O, 25.31%. Found: C, 70.6; H, 4.2; O, 25.4%.

8.3.6. (Benzyloxy)phenyl)methylene)bis(4-hydroxy-2H-chromen-2-one) (**2f**). Yield: 87%; m.p. 264 °C. IR ν (cm^{-1}): 3072 (OH); 1665 (CO); 1547 (C=C). 1H NMR (400 MHz, $CDCl_3$) (λ , ppm): 6.12 (s, 1H, H_{12}); 7.13 (dd, 2H, $H_{29,25}$), 7.45–7.48 (m, 6H, $H_{9,21,8,20,7,19}$); 7.65 (td, 2H, $H_{28,26}$); 8.06 (dd, 2H, $H_{10,22}$), 11.35 (s, 1H, H_{23}), 11.56 (s, 1H, H_{31}). ^{13}C NMR (100 MHz, $CDCl_3$) (λ , ppm): 36.21 (C_{12}); 103.75 ($C_{3,13}$); 106.34 (C_5); 116.82 (C_{17}); 120.95 (C_7); 124.54 (C_{19}); 125.14 (C_{27}); 128.45 ($C_{10,22}$); 131.74 ($C_{9,21}$), 133.27 ($C_{8,20}$); 134.46 ($C_{29,25}$); 152.45 ($C_{28,26}$); 152.65 (C_{24}); 164.75 ($C_{6,16}$); 166.18 (C_2), 166.96 (C_{14}), 169.38 ($C_{4,18}$). Calcd for $C_{32}H_{22}O_7$: C, 74.12%; H, 4.28%; O, 21.60%. Found: C, 74.2; H, 4.3; O, 21.7%.

8.3.7. 3,3'-((4-Nitrophenyl)methylene)bis(4-hydroxy-2H-chromen-2-one) (**2g**). Yield: 85%; m.p. 226 °C. IR ν (cm^{-1}): 3075 (OH); 1641 (CO); 1565 (C=C). 1H NMR (400 MHz, $CDCl_3$) (λ , ppm): 1.37 (t, 3H, H_c), 3.97 (q, 2H, H_b), 6.17 (s, 1H, H_{12}); 6.54–6.75 (m, 2H, $H_{29,25}$), 6.85 (d, 1H, H_{28}); 7.45 (d, 4H, $H_{9,21,7,19}$); 7.65 (td, 2H, $H_{8,20}$), 8.31 (s, 2H, $H_{10,22}$), 11.43 (d, 2H, $H_{23,31}$). ^{13}C NMR (100 MHz, $CDCl_3$) (λ , ppm): 14.74 (C_c); 35.95 (C_{12}); 64.85 (C_b); 110.65 ($C_{3,13}$); 114.54 ($C_{28,25}$); 116.76 ($C_{5,17,7,19}$); 119.65 ($C_{29,10,22}$); 124.57 ($C_{9,21,8,20}$); 125.12 (C_{24}); 126.78 (C_{27}), 132.96 (C_{26}); 144.95 ($C_{2,14}$); 146.16 ($C_{6,16}$); 152.56 ($C_{4,18}$). Calcd for $C_{25}H_{15}O_8N$: C, 65.65%; H, 3.31%; O, 27.98%. Found: C, 65.7; H, 3.4; O, 27.9%.

8.4. General Procedure for the Synthesis of Substituted Coumarin Derivatives 3–4. A mixture of 4-hydroxycoumarin (4 equiv) and isophthalaldehyde (1 equiv) or terephthalaldehyde (1 equiv) was mixed and placed in a round bottom flask, and the mixture was heated at reflux in EtOH for 4 h. The reaction mixture was allowed to cool at room temperature and filtered off. The residue was then boiled with absolute ethanol (20 mL) and filtered hot. It was

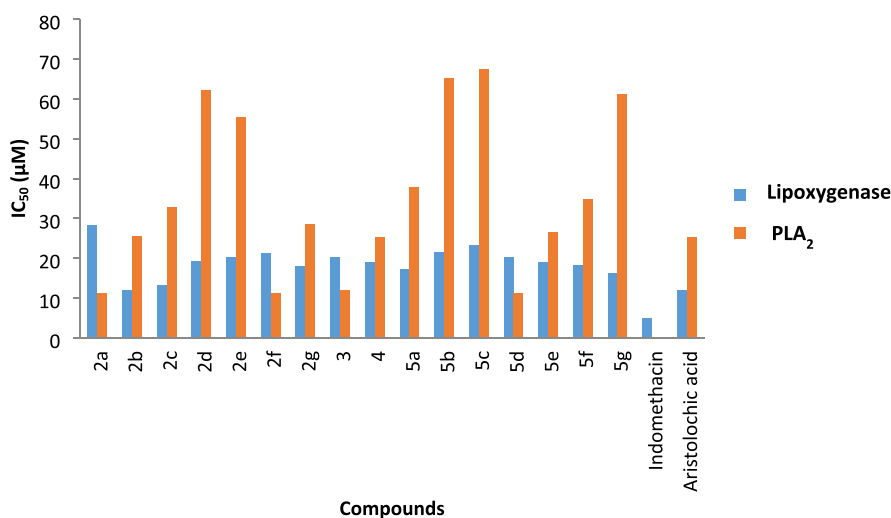


Figure 11. IC_{50} values of compounds 2–5 for anti-inflammatory activity.

recrystallized with acetone and absolute alcohol to afford the target coumarin derivatives 3–4.

8.4.1. Coumarin Derivative 3. Yield: 85%; m.p. 236 °C. IR ν (cm⁻¹): 3065 (OH); 1645 (CO); 1567 (C=C). ¹H NMR (300 MHz, DMSO-*d*₆) δ 8.32 (s, 4H, OH), 7.89–7.02 (m, 20H, CH arom), 6.31 (s, 2H, CH).

8.4.2. Coumarin Derivative 4. Yield: 90%; m.p. 245 °C. IR ν (cm⁻¹): 3055 (OH); 1643 (CO); 1567 (C=C). ¹H NMR (300 MHz, DMSO-*d*₆) δ 8.32 (s, 4H, OH), 7.89–7.02 (m, 20H, CH arom), 6.31 (s, 2H, CH).

8.5. Synthesis of Epoxydicoumarins 5. Dicoumarol 2 was heated in acetic anhydride until it was dissolved. The reaction mixture was heated to a boil for 2 h and then chilled for 24 h before the precipitate was filtered out and dried.

8.5.1. 7-(3-Ethoxy-4-hydroxyphenyl)-6H,7H,8H-pyrano[3,2-c:5,6-c']dichromene-6,8-dione (5a). Yield: 95%; m.p. 267 °C. IR ν (cm⁻¹): 1665 (CO); 1575 (C=C). ¹H NMR (400 MHz, CDCl₃) (λ , ppm): 1.14 (t, 3H, H_b); 2.52 (q, 2H, H_a); 5.16 (s, 1H, H₁₂); 7.12 (d, 2H, H_{28,26}), 7.35–7.42 (m, 4H, H_{29,25,7,19}); 7.46 (t, 2H, H_{9,21}); 7.65 (td, 2H, H_{8,20}), 8.11 (dd, 2H, H_{10,22}). ¹³C NMR (100 MHz, CDCl₃) (λ , ppm): 15.45 (C_b); 28.63 (C_a); 34.65 (C₁₂); 106.67 (C_{3,13}); 113.64 (C_{5,17}); 117.23 (C_{7,19}); 122.47 (C_{10,22}); 124.75 (C_{9,21}); 128.25 (C₂₈); 128.94 (C₂₆); 132.85 (C_{8,7}); 138.46 (C_{29,25}); 143.82 (C_{24,27}); 152.85 (C_{6,16}); 153.54 (C_{4,18}); 160.35 (C_{2,14}). Calcd for C₂₇H₁₈O₇: C, 71.36%; H, 3.99%; O, 24.65%. Found: C, 71.4; H, 4.1; O, 24.7%.

8.5.2. 7-(*p*-Tolyl)-6H,7H,8H-pyrano[3,2-c:5,6-c']dichromene-6,8-dione (5b). Yield: 90%; m.p. 256 °C. IR ν (cm⁻¹): 1665 (CO); 1564 (C=C). ¹H NMR (400 MHz, CDCl₃) (λ , ppm): 2.28 (s, 3H, H_a); 5.14 (s, 1H, H₁₂); 7.12 (d, 2H, H_{28,27}), 7.35 (d, 2H, H_{26,29}); 7.35 (d, 2H, H_{7,19}); 7.42 (t, 2H, H_{9,21}); 7.56 (td, 2H, H_{8,20}), 8.13 (dd, 2H, H_{10,22}). ¹³C NMR (100 MHz, CDCl₃) (λ , ppm): 21.27 (C_a); 34.62 (C₁₂); 106.63 (C_{3,13}); 113.64 (C_{5,17}); 117.32 (C_{7,19}); 122.47 (C₂₈); 124.75 (C_{10,22}); 128.93 (C₂₉); 129.45 (C_{9,21}); 132.86 (C₂₇), 137.48 (C_{8,20}); 138.23 (C_{24,26,25}); 152.76 (C_{6,16}); 153.45 (C_{4,18}); 160.31 (C_{2,14}). Calcd for C₂₅H₁₃O₅Br: C, 63.45%; H, 2.77%; O, 16.90%. Found: C, 63.5; H, 2.8; O, 17.1%.

8.5.3. 7-(3,4-Dimethoxyphenyl)-6H,7H,8H-pyrano[3,2-c:5,6-c']dichromene-6,8-dione (5c). Yield: 78%; m.p. 262 °C. IR ν (cm⁻¹): 1667 (CO); 1485 (C=C). ¹H NMR (400 MHz, CDCl₃) (λ , ppm): 4.82 (s, 1H, H₁₂); 7.35 (d, 2H, H_{29,25}), 7.45 (d, 2H, H_{28,26}); 7.52–7.56 (m, 4H, H_{9,21,7,19}); 7.61 (td, 2H, H_{8,20}), 8.35 (dd, 2H, H_{10,22}). ¹³C NMR (100 MHz, CDCl₃) (λ , ppm): 51.65 (C₁₂); 122.25 (C_{3,13}); 130.42 (C_{5,17,7,19}); 134.15 (C_{10,22}); 140.75 (C_{9,21,8,20}); 142.45 (C_{28,26}); 145.56 (C_{29,25}); 148.35 (C₂₇); 150.75 (C₂₄), 169.56 (C_{6,16}); 170.85 (C_{4,18}); 177.21 (C_{2,14}). Calcd for C₂₇H₁₈O₈: C, 68.94%; H, 3.86%; O, 27.21%. Found: C, 69.1; H, 3.9; O, 27.3%.

8.5.4. 7-Phenyl-6H,7H,8H-pyrano[3,2-c:5,6-c']dichromene-6,8-dione (5d). Yield: 94%; m.p. 287 °C. IR ν (cm⁻¹): 1658 (CO); 1585 (C=C). ¹H NMR (400 MHz, CDCl₃) (λ , ppm): 3.52 (s, 3H, H_d); 3.67 (s, 3H, H_b); 5.13 (s, 1H, H₁₂); 6.35 (d, 1H, H₂₈), 6.52 (dd, 1H, H₂₆); 7.35 (d, 2H, H_{7,19}); 7.45 (td, 2H, H_{9,21}), 7.54 (d, 1H, H₂₉), 7.65 (td, 2H, H_{8,20}), 8.17 (dd, 2H, H_{10,22}). ¹³C NMR (100 MHz, CDCl₃) (λ , ppm): 31.45 (C₁₂); 55.46 (C_d); 55.62 (C_b); 99.35 (C₂₆); 104.58 (C_{3,13}); 104.62 (C₂₈); 113.85 (C₂₄); 117.22 (C_{5,17}); 120.18 (C_{7,19}); 122.17 (C_{10,22}); 124.46 (C_{9,21}), 132.32 (C_{8,20}); 133.38 (C₂₉); 152.72 (C_{6,16}); 154.21 (C₂₇); 159.42 (C₂₅); 160.42 (C_{4,18}), 162.85 (C_{2,14}). Calcd for C₂₅H₁₄O₅: C,

76.14%; H, 3.58%; O, 20.28%. Found: C, 76.2; H, 3.6; O, 20.3%.

8.5.5. 7-(4-Methoxyphenyl)-6H,7H,8H-pyrano[3,2-c:5,6-c']dichromene-6,8-dione (5e). Yield: 85%; m.p. 287 °C. IR ν (cm⁻¹): 1665 (CO); 1607 (C=C). ¹H NMR (400 MHz, CDCl₃) (λ , ppm): 5.12 (s, 1H, H₁₂); 7.41–7.47 (6, 4H, H_{9,21,7,19}), 7.73–7.70 (m, 4H, H_{8,20,29,25}); 8.21 (d, 2H, H_{10,22}); 8.31 (dd, 1H, H_{28,26}). ¹³C NMR (100 MHz, CDCl₃) (λ , ppm): 34.01 (C₁₂); 105.22 (C_{3,13}); 112.94 (C_{5,17}); 116.72 (C_{7,19}); 123.26 (C_{10,22}); 123.46 (C_{28,26}); 125.01 (C_{9,21}); 130.56 (C_{29,25}); 133.51 (C_{8,20}), 146.71 (C₂₇); 148.73 (C₂₄); 152.12 (C_{6,16}); 153.64 (C_{4,18}); 159.64 (C_{2,14}). Calcd for C₂₆H₁₆O₆: C, 73.58%; H, 3.80%; O, 22.62%. Found: C, 73.6; H, 3.9; O, 22.7%.

8.5.6. 7-(2-(Benzyloxy)phenyl)-6H,7H,8H-pyrano[3,2-c:5,6-c']dichromene-6,8-dione (5f). Yield: 87%; m.p. 324 °C. IR ν (cm⁻¹): 1664 (CO); 1607 (C=C). ¹H NMR (400 MHz, CDCl₃) (λ , ppm): 5.14 (s, 1H, H₁₂); 7.35–7.51 (m, 8H, H_{9,21,8,20,7,19,29,25}), 7.67 (t, 2H, H_{28,26}); 8.12 (d, 2H, H_{10,22}). ¹³C NMR (100 MHz, CDCl₃) (λ , ppm): 34.38 (C₁₂); 106.64 (C_{3,13}); 113.14 (C_{5,17}); 117.12 (C_{7,19}); 122.32 (C₂₇); 124.56 (C_{10,22}); 130.48 (C_{9,21}); 131.42 (C_{8,20}); 132.74 (C_{29,25}), 139.78 (C_{28,26,24}); 152.52 (C_{6,16}); 153.62 (C_{4,18}); 159.74 (C_{2,14}). Calcd for C₃₂H₂₀O₆: C, 76.79%; H, 4.03%; O, 19.18%. Found: C, 76.8; H, 4.1; O, 19.2%.

8.5.7. 7-(4-Nitrophenyl)-6H,7H,8H-pyrano[3,2-c:5,6-c']dichromene-6,8-dione (5g). Yield: 95%; m.p. 284 °C. IR ν (cm⁻¹): 1664 (CO); 1624 (C=C). ¹H NMR (400 MHz, CDCl₃) (λ , ppm): 1.38 (t, 3H, H_c), 4.12 (q, 2H, H_b), 5.21 (s, 1H, H₁₂); 6.65 (dd, 1H, H₂₉), 6.76 (d, 1H, H₂₅); 7.38 (d, 1H, H₂₆); 7.84 (dd, 2H, H_{9,21}), 7.56 (td, 2H, H_{7,19}), 7.72 (td, 2H, H_{8,20}), 8.12 (dd, 2H, H_{10,22}). ¹³C NMR (100 MHz, CDCl₃) (λ , ppm): 14.83 (C_c); 34.57 (C₁₂); 64.62 (C_b); 106.32 (C_{3,13}); 114.52 (C₂₉); 115.47 (C₂₆); 117.33 (C₂₇); 119.68 (C_{5,17}); 122.34 (C_{7,19}); 122.64 (C₂₅); 124.82 (C_{10,22}), 133.13 (C_{9,21}); 139.47 (C_{8,20}); 139.72 (C₂₄); 150.45 (C₂₇), 152.75 (C₂₈), 155.73 (C_{6,16}); 160.37 (C_{4,18}); 169.12 (C_{2,14}). Calcd for C₂₅H₁₃O₇N: C, 68.34%; H, 2.98; N, 3.19; %; O, 25.49%. Found: C, 68.4; H, 3.1; N, 3.2; O, 25.5%.

9. ANTIBACTERIAL ACTIVITY

9.1. Bacterial Strains, Media, and Growth Conditions.

Bacteria strains used as indicator microorganisms for the antibacterial activity assays were: *Micrococcus luteus* (*M. luteus*) LB 14110, *Staphylococcus aureus* (*S. aureus*) ATCC 6538, *Listeria monocytogenes* (*L. monocytogenes*) ATCC 19117, *Salmonella Typhimurium* (*S. typhimurium*) ATCC 14028, *Pseudomonas aeruginosa* (*P. aeruginosa*) ATCC 49189, and *>E. coli<*. These bacterial strains were grown overnight in Luria-Bertani (LB) agar medium (g/L): peptone 10; yeast extract 5 and NaCl 5 at pH 7.2 under aerobic conditions and constant agitation (200 rpm) at 30 °C for *M. luteus* LB14110 and *L. monocytogenes* ATCC 19117 and at 37 °C for *S. aureus* ATCC 6538, *S. typhimurium* ATCC 14028 and *P. aeruginosa* ATCC 49189 and then diluted 1:100 in LB media and incubated for 5 h under constant agitation (200 rpm) at the appropriate temperature.

9.2. Agar Well Diffusion Method. Agar well diffusion method was employed for the determination of the antimicrobial activity of the synthesized compounds according to Güven et al.³¹ with some modifications. Briefly, the synthesized compounds are allowed to diffuse out into the appropriate agar medium (LB agar medium) and interact in a

plate freshly seeded with a suspension of the indicator microorganisms (0.1 mL of 10⁸ cells per mL). The plate was incubated at the appropriate temperature after staying at 4 °C for 2 h. The resulting zones of inhibition will be uniformly circular as there will be a confluent lawn of growth. The antibacterial activity was assayed by measuring in millimeters the diameter of the inhibition zone formed around the well. All tests are assayed in triplicate and expressed as the average \pm standard deviation of the measurements.

9.3. Minimum Inhibitory Concentration (MIC). The minimum inhibitory concentration (MIC) of the synthesized compounds was determined by NCCLS guideline M7-A6 and M38-P (National Committee for clinical laboratory standard, Wayne 1998).³² The test was performed in sterile 96-well microplates with a final volume in each microplate well of 100 μ L. The synthesized compounds (20 mg/mL) were properly prepared in solution of dimethylsulfoxide (DMSO)/water (1/9; v/v). The inhibitory activity of each synthesized compound was transferred to each well to obtain a twofold serial dilution of the original sample and visible growth after incubation. As an indicator of microorganism growth, 25 μ L of thiazolyl blue tetrazolium bromide (MTT), indicator solution (0.5 mg/mL) dissolved in sterile water was added to the wells and incubated at room temperature for 30 min. This determination was done in triplicate, and the obtained results were very similar. The reported value is the average of the three tests.

10. ANTIOXIDANT ACTIVITY

10.1. DPPH Radical Scavenging Assay. The free radical scavenging activity for DPPH radicals was performed as described previously.³³ In brief, the reaction mixture contained 200 μ L of 0.1 mM DPPH–ethanol solution, 90 μ L of 50 mM Tris–HCl buffer (pH 7.4), and 10 μ L of deionized water (as control) and various concentrations of the compounds 2–5 (3.0–16.0 μ M), and ascorbic acid was used as a control. The reaction mixture was incubated for 30 min at room temperature, and absorbance was read at 540 nm. The percentage radical scavenging activity was calculated according to the following formula: inhibition (%) = [(absorbance control – absorbance sample)/absorbance control] \times 100.

11. ANTI-INFLAMMATORY ACTIVITY

11.1. Lipoxigenase Inhibition Assay. The lipoxigenase inhibition assay was performed according to the method previously described.^{34,35} Briefly, to a solution of 0.1 mL of 0.2 M borate buffer (pH 9.0) and 0.1 mL of 1000 units lipoxylase enzyme solution, the compounds 2–5 tested and dissolved in DMSO (3–16 μ M) were added, agitated, and incubated at room temperature for 5 min. Later, 2.0 mL of 0.6 mM linoleic acid was added and the absorbance was measured at 234 nm. Indomethacin was used as standard. The percent (%) inhibition was calculated by the following equation:

$$\text{inhibition (\%)} = \frac{[(\text{absorbance control} - \text{absorbance sample}) / \text{absorbance control}] \times 100}{1}$$

11.2. Indirect Haemolytic Assay. Indirect haemolytic assay was performed according to the reported method.^{36,37} One milliliter of fresh human red blood cells and 1 mL of fresh Hen's egg yolk in 8 mL of phosphate buffered saline were mixed to prepare the substrate for indirect hemolytic activity.

One milliliter of this suspension was incubated with 4–28 μ g of partially purified venom for 45 min at 37 °C, and 9 mL ice cold sodium perborate was used to stop the reaction. The reaction mixture was centrifuged at 2000 rpm for 20 min, and then the released hemoglobin was read at 540 nm. For inhibition studies, 10 μ g of the venom sample (secretory PLA₂ purchased from Sigma) was incubated with various concentrations of compounds 2–5 (20–100 μ M in DMSO) for 30 min at room temperature and mixed with 1 mL of substrate solution and incubated at room temperature for 30 min. The reaction was stopped by adding 9 mL of ice cold sodium perborate, and the extent of hemolysis is measured at 540 nm. Aristolochic acid was used as reference drug. The percent (%) inhibition was calculated as follows: inhibition (%) = [(absorbance control – absorbance sample)/absorbance control] \times 100.

12. THEORETICAL DETAILS

Molecular docking simulation of the synthesized compounds 2a–f and 5a–e into antibacterial protein targets is carried out using the Molecular Operating Environment (MOE 2015.10) software package.³⁸ The antibacterial targets (PDB IDs: 1JJI, 1JIL, 1LXC, 2WFG, 3JQ9, 5R80, and 6CJF) are retrieved from the protein data bank.³⁹

Each protein target was 3D protonated, with default parameters of MOE, after removing solvent molecules and co-crystallized ligands and adding the missing hydrogen atoms. Further, the errors like steric clashes, missing loops, missing atom names, and picking alternate conformations in the protein crystallographic data were corrected. Then, the energy minimization was performed using the MMFF94x force field and the partial charges were assigned using the default parameters. The studied ligands are drawn and minimized with the MOE package using the same force field. The active site, where docking was carried out, is determined by using the Site Finder application in MOE. The dummy site was created with an alpha sphere around an active site. The default triangle matcher placement method was employed for docking. London dG scoring function was chosen to score the top 1000 poses obtained from the triangle matcher placement method. The 100 top-ranked poses are ranked by the London dG and then minimized using the MMFF94x force field within a rigid receptor.

The resulting poses were then scored using the generalized-Born volume integral/weighted surface area (GBVI/WSA) dG scoring function, which estimates the binding free energy for a given pose of the ligand. The docking score is the binding free energy, calculated by the GBVI/WSA scoring function in the S field, which is the score of the last stage. The lower score indicates a more favorable pose. Poses with high RMSD values are not considered. The ligand interaction tool was used for 2D and 3D visualizations of protein–ligand interactions.

■ ASSOCIATED CONTENT

Data Availability Statement

The datasets generated during and/or analyzed during the current study are available from the corresponding author on reasonable request.

Supporting Information

The Supporting Information is available free of charge at <https://pubs.acs.org/doi/10.1021/acsomega.2c06802>.

(Figure S1) FT-IR spectrum of compound **2a**, (Figure S2) ^1H NMR spectrum of compound **2a** (in CDCl_3 , 400 MHz, 25 °C, TMS), (Figure S3) ^{13}C NMR spectrum of compound **2a** (in CDCl_3 , 125 MHz, 25 °C, TMS), (Figure S4) MS Spectra of compound **2a**, (Figure S5) FT-IR spectrum of compound **2b**, (Figure S6) ^1H NMR spectrum of compound **2b** (in CDCl_3 , 400 MHz, 25 °C, TMS), (Figure S7) ^{13}C NMR spectrum of compound **2b** (in CDCl_3 , 125 MHz, 25 °C, TMS), (Figure S8) MS Spectra of compound **2b**, (Figure S9) FT-IR spectrum of compound **2c**, (Figure S10) ^1H NMR spectrum of compound **2c** (in CDCl_3 , 400 MHz, 25 °C, TMS), (Figure S11) ^{13}C NMR spectrum of compound **2c** (in CDCl_3 , 125 MHz, 25 °C, TMS), (Figure S12) MS spectra of compound **2c**, (Figure S13) FT-IR spectrum of compound **2d**, (Figure S14) ^1H NMR spectrum of compound **2d** (in CDCl_3 , 400 MHz, 25 °C, TMS), (Figure S15) ^{13}C NMR spectrum of compound **2d** (in CDCl_3 , 125 MHz, 25 °C, TMS), (Figure S16) MS spectra of compound **2d**, (Figure S17) FT-IR spectrum of compound **2e**, (Figure S18) ^1H NMR spectrum of compound **2e** (in CDCl_3 , 400 MHz, 25 °C, TMS), (Figure S19) ^{13}C NMR spectrum of compound **2e** (in CDCl_3 , 125 MHz, 25 °C, TMS), (Figure S20) MS spectra of compound **2e**, (Figure S21) FT-IR spectrum of compound **2f**, (Figure S22) ^1H NMR spectrum of compound **2f** (in CDCl_3 , 400 MHz, 25 °C, TMS), (Figure S23) ^{13}C NMR spectrum of compound **2f** (in CDCl_3 , 125 MHz, 25 °C, TMS), (Figure S24) MS spectra of compound **2f**, (Figure S25) FT-IR spectrum of compound **2g**, (Figure S26) ^1H NMR spectrum of compound **2g** (in CDCl_3 , 400 MHz, 25 °C, TMS), (Figure S27) ^{13}C NMR spectrum of compound **2g** (in CDCl_3 , 125 MHz, 25 °C, TMS), (Figure S28) MS spectra of compound **2g**, (Figure S29) FT-IR spectrum of compound **5a**, (Figure S30) ^1H NMR spectrum of compound **5a** (in CDCl_3 , 400 MHz, 25 °C, TMS), (Figure S31) ^{13}C NMR spectrum of compound **5a** (in CDCl_3 , 125 MHz, 25 °C, TMS), (Figure S32) MS spectra of compound **5a**, (Figure S33) FT-IR spectrum of compound **5b**, (Figure S34) ^1H NMR spectrum of compound **5b** (in CDCl_3 , 400 MHz, 25 °C, TMS), (Figure S35) ^{13}C NMR spectrum of compound **5b** (in CDCl_3 , 125 MHz, 25 °C, TMS), (Figure S36) MS spectra of compound **5b**, (Figure S37) FT-IR spectrum of compound **5c**, (Figure S38) ^1H NMR spectrum of compound **5c** (in $\text{DMSO}-d_6$, 400 MHz, 25 °C, TMS), (Figure S39) ^{13}C NMR spectrum of compound **5c** (in $\text{DMSO}-d_6$, 125 MHz, 25 °C, TMS), (Figure S40) MS Spectra of compound **5c**, (Figure S41) FT-IR spectrum of compound **5d**, (Figure S42) ^1H NMR spectrum of compound **5d** (in CDCl_3 , 400 MHz, 25 °C, TMS), (Figure S43) ^{13}C NMR spectrum of compound **5d** (in CDCl_3 , 125 MHz, 25 °C, TMS), (Figure S44) MS spectra of compound **5d**, (Figure S45) FT-IR spectrum of compound **5g**, (Figure S46) ^1H NMR spectrum of compound **5g** (in $\text{DMSO}-d_6$, 400 MHz, 25 °C, TMS), (Figure S47) ^{13}C NMR spectrum of compound **5g** (in $\text{DMSO}-d_6$, 125 MHz, 25 °C, TMS), (Figure S48) MS spectra of compound **5g**, (Figure S49) FT-IR spectrum of compound **5e**, (Figure S50) ^1H NMR spectrum of compound **5e** (in CDCl_3 , 400 MHz, 25 °C, TMS), (Figure S51) ^{13}C NMR spectrum of compound **5e** (in

CDCl_3 , 125 MHz, 25 °C, TMS), (Figure S52) MS spectra of compound **5e**, (Figure S53) FT-IR spectrum of compound **5f**, (Figure S54) ^1H NMR spectrum of compound **5g** (in CDCl_3 , 400 MHz, 25 °C, TMS), (Figure S55) ^{13}C NMR spectrum of compound **5g** (in CDCl_3 , 125 MHz, 25 °C, TMS), (Figure S56) MS spectra of compound **5g**, (Figure S57) ^1H NMR spectrum of compound **3** (in CDCl_3 , 400 MHz, 25 °C, TMS), (Figure S58) FT-IR spectrum of compound **3**, (Figure S59) ^1H NMR spectrum of compound **4** (in CDCl_3 , 400 MHz, 25 °C, TMS), (Figure S60) FT-IR spectrum of compound **4** (PDF)

AUTHOR INFORMATION

Corresponding Authors

Aziza Mnasri – Research Laboratory of Environmental Sciences and Technologies (LR16ES09), Higher Institute of Environmental Sciences and Technology, University of Carthage, Hammam-Lif PB 77, Tunisia; Email: azizamnasri10@gmail.com

Naceur Hamdi – Department of chemistry, College of Science and Arts at ArRass, Qassim University, ArRass 51921, Saudi Arabia; Research Laboratory of Environmental Sciences and Technologies (LR16ES09), Higher Institute of Environmental Sciences and Technology, University of Carthage, Hammam-Lif PB 77, Tunisia; orcid.org/0000-0003-0110-9588; Phone: +966556394839; Email: naceur.hamdi@isste.rnu.tn

Authors

Nasser Amri – Department of Chemistry, Faculty of Science, Jazan University, Jazan 45142, Saudi Arabia

Houcine Ghalla – Quantum and Statistical Physics Laboratory, University of Monastir, Monastir 5000, Tunisia

Rafik Gatri – Laboratoire de Synthèse Organique Sélective et Hétérocyclique Évaluation Biologique LR17ES01 Faculté des Sciences de Tunis Faculté des Sciences de Tunis Campus Universitaire 1092, Université de Tunis El Manar, Tunis 1092, Tunisia

Complete contact information is available at:

<https://pubs.acs.org/10.1021/acsomega.2c06802>

Funding

The authors declare that no funds, grants, or other support were received during the preparation of this manuscript.

Notes

The authors declare no competing financial interest.

ACKNOWLEDGMENTS

Researchers would like to thank the Deanship of Scientific Research, Qassim University for funding publication of this project.

REFERENCES

- (1) Karimi, A. R.; Sedaghatpour, F. Novel mono- and bis(spiro-2-amino-4H-pyrans): alum-catalyzed reaction of 4-hydroxycoumarin and malononitrile with isatins, quinones, or ninhydrin. *Synthesis* **2010**, *2010*, 1731–1735.
- (2) Musa, M.; Cooperwood, J.; Khan, M. O. F. A review of coumarin derivatives in pharmacotherapy of breast cancer. *Curr. Med. Chem.* **2008**, *15*, 2664–2679.

- (3) Kontogiorgis, C.; Detsi, A.; Hadjipavlou-Litina, D. Coumarin-based drugs: a patent review (2008 - present). *Expert Opin. Ther. Pat.* **2012**, *22*, 437–454.
- (4) Lin, Y.; Shen, X.; Yuan, Q.; Yan, Y. Microbial biosynthesis of the anticoagulant precursor 4-hydroxycoumarin. *Nat. Commun.* **2013**, *4*, 3603.
- (5) Beinema, M.; Brouwers, J. R. B. J.; Schalekamp, T.; Wilffert, B. Pharmacogenetic differences between warfarin, acenocoumarol and phenprocoumon. *Thromb. Haemostasis* **2008**, *100*, 1052–1057.
- (6) Madari, H.; Panda, D.; Wilson, L.; Jacobs, R. S. A unique microtubule stabilizing natural product that is synergistic with taxol. *Cancer Res.* **2003**, *63*, 1214–1220.
- (7) Cherkupally, S. R.; Mekala, R. Synthesis of novel 6,6-methylenebis-[3-(2-anilinoacetyl)-4-hydroxycoumarin] derivatives. *Chem. Pharm. Bull.* **2008**, *56*, 1732–1734.
- (8) Bellis, D. M.; Spring, M. S.; Stoker, J. R. The biosynthesis of dicoumarol. *Biochem. J.* **1967**, *103*, 202–206.
- (9) (a) Hamdi, N.; Puerta, M. C.; Valerga, P. Synthesis, structure, antimicrobial and antioxidant investigations of dicoumarol and related compounds. *Eur. J. Med. Chem.* **2008**, *43*, 2541–2548. (b) Karmakar, B.; Nayak, A.; Banerji, J. Sulfated titania catalyzed water mediated efficient synthesis of dicoumarols. A green approach. *Tetrahedron Lett.* **2012**, *53*, 4343–4346.
- (10) (a) Kolos, N. N.; Gozalishvili, L. L.; Yaremenko, F. G.; Shishkin, O. V.; Shishkina, S. V.; Konovalova, I. S. Aroylbis(4-hydroxycoumarin-3-yl)methanes in reactions with 1,2-diaminobenzenes. *Russ. Chem. Bull.* **2007**, *56*, 2277–2283. (b) Sadeghi, B. Synthesis of silica-supported perchloric acid nanoparticles (HClO₄-SiO₂ NPs). Efficient synthesis of biscoumarin derivatives in water. *J. Chem. Res.* **2013**, *37*, 171–173.
- (11) Siddiqui, Z. N.; Farooq, F. Zn(Proline)₂: a novel catalyst for the synthesis of dicoumarols. *Catal. Sci. Technol.* **2011**, *1*, 810–816.
- (12) Ziarani, G. M.; Hajiabbasi, P. Recent application of 4-hydroxycoumarin in multi-component reactions. *Heterocycles* **2013**, *87*, 1415–1439.
- (13) Weinmann, I. History of the development and applications of coumarin and coumarin-related compounds. In *Coumarins: Biology, Applications and Mode of Action*; O’Kennedy, R.; Thornes, R.D. Eds.; John Wiley & Sons, Inc.: Los Angeles, CA, USA, 1997, 1–22.
- (14) Marcu, M. G.; Schulte, W. T.; Neckers, L. Novobiocin and related coumarins and depletion of heat shock protein 90-dependent signaling proteins. *J. Natl. Cancer Inst.* **2000**, *92*, 242–248.
- (15) Borges, F.; Roleira, F.; Milhazes, N.; Santana, L.; Uriarte, E. Simple coumarins and analogues in medicinal chemistry: Occurrence, synthesis and biological activity. *Curr. Med. Chem.* **2005**, *12*, 887–916.
- (16) Chiang, C. C.; Hsu, L. Y.; Tsai, H. J.; Yao, C. W.; Chang, T. C. Synthesis and antimicrobial evaluation of coumarin derivatives. *J. Chiong Chang Inst. Technol.* **2008**, *37*, 15–22.
- (17) Cavar, S.; Kovač, F.; Maksimović, M. Synthesis and antioxidant activity of selected 4-methylcoumarins. *Food Chem.* **2009**, *117*, 135–142.
- (18) Jung, J. C.; Park, O. S. Synthetic approaches and biological activities of 4-hydroxycoumarin derivatives. *Molecules* **2009**, *14*, 4790–4803.
- (19) Symeonidis, T.; Chamilos, M.; Hadjipavlou-Litina, D. J.; Kallitsakis, M.; Litinas, K. E. Synthesis of hydroxycoumarins and hydroxybenzo[f]- or [h]coumarins as lipid peroxidation inhibitors. *Bioorg. Med. Chem. Lett.* **2009**, *19*, 1139–1142.
- (20) Kostova, I. Studying plant-derived coumarins for their pharmacological and therapeutic properties as potential anticancer drugs. *Expert Opin. Drug Disc.* **2007**, *2*, 1605–1618.
- (21) Nolan, A. K.; Doncaster, R. J.; Dunstan, S. M.; Scot, A. K.; Frenkel, D.; Siegel, D.; Ross, D.; Barnes, J.; Levy, C.; Leys, D.; et al. Synthesis and biological evaluation of coumarin-based inhibitors of NAD(P)H: quinone oxidoreductase-1 (NQO1). *J. Med. Chem.* **2009**, *52*, 7142–7156.
- (22) Mahajan, D. H.; Pannecouque, C.; De Clercq, E.; Chikhalia, K. H. Synthesis and studies of new 2-(coumarin-4-yloxy)-4,6-(substituted)-s-triazine derivatives as potential anti-HIV agents. *Arch. Pharm.* **2009**, *342*, 281–290.
- (23) Zhao, H.; Neamati, N.; Hong, H.; Mazumder, A.; Wang, S.; Sunder, S.; Milne George, W. A.; Pommier, Y.; Burke, T. R., Jr. Coumarin-based inhibitors of HIV integrase. *J. Med. Chem.* **1997**, *40*, 242–249.
- (24) Hooper, D. C.; Wolfson, J. S.; McHugh, G. L.; Winters, M. B.; Swartz, M. N. Effects of novobiocin, coumermycin A1, clorobiocin, and their analogs on Escherichia coli DNA gyrase and bacterial growth. *Antimicrob. Agents Chemother.* **1982**, *22*, 662–671.
- (25) Pan, Y.; Liu, T.; Wang, X.; Sun, J. Research progress of coumarins and their derivatives in the treatment of diabetes. *J. Enzyme Inhib. Med. Chem.* **2022**, *37*, 616–628.
- (26) Slimani, I.; Hamzaoui, S.; Mansour, L.; Harrath, A. H.; Hamdi, N. One-pot, simple and efficient synthesis of novel bioactive 4-aryl-1,2-dihydro-6-(4-hydroxy-2-oxo-2H-chromen-3-yl)-2-oxopyridin-3-carbonitriles via multi-component approach. *J. King Saud Univ. – Sci.* **2020**, *32*, 1212–1217.
- (27) Le Bras, G.; Hamze, A.; Messaoudi, S.; Provot, O.; Le Calvez, P.-B.; Brion, J.-D.; Alami, M. Synthesis of isocoumarin via pTSA-catalyzed annulation of diarylalkynes. *Synthesis* **2008**, *10*, 1607–1611.
- (28) da Silva, C. R. B.; Gonçalves, V. L. C.; Lachter, E. R.; Mota, C. J. A. Etherification of glycerol with benzyl alcohol catalyzed by solid acids. *J. Braz. Chem. Soc.* **2009**, *20*, 201–204.
- (29) Mobinikhaledi, A.; Moghanian, H.; Deinavizadeh, M. pTSA-catalyzed condensation of xylenols and aldehydes under solvent-free conditions: one-pot synthesis of 9H-xanthene or bisphenol derivatives. *C. R. Chimie.* **2013**, *16*, 1035–1041.
- (30) (a) Chanda, A.; Fokin, V. V. Organic synthesis “on water”. *Chem. Rev.* **2009**, *109*, 725–748. (b) Heravi, M. M.; Sadjadi, S.; Mokhtari Haj, N.; Oskooie, H. A.; Bamoharram, F. F. Role of various heteropolyacids in the reaction of 4-hydroxycoumarin, aldehydes and ethylcyanoacetate. *Catal. Commun.* **2009**, *10*, 1643–1646.
- (31) Güven, K.; Yücel, E.; Cetintaş, F. Antimicrobial activities of fruits of Crataegus and Pyrus. Species. *Pharm. Biol.* **2006**, *44*, 79–83.
- (32) Sellem, I.; Kaaniche, F.; Chakchouk, A. M.; Mellouli, L. Antioxidant, antimicrobial and anti-acetylcholinesterase activities of organic extracts from aerial parts of three Tunisian plants and correlation with polyphenols and flavonoids contents. *Bangladesh J. Pharm.* **2016**, *11*, 531–544.
- (33) Kirby, A. J.; Schmidt, R. J. The antioxidant activity of Chinese herbs for eczema and of placebo herbs. *I. J. Ethnopharmacol.* **1997**, *56*, 103–108.
- (34) Re, R.; Pellegrini, N.; Proteggente, A.; Pannala, A.; Yang, M.; Rice-Evans, C. Antioxidant activity applying an improved ABTS radical cation decolorization assay. *Free Radical Biol. Med.* **1999**, *26*, 1231–1237.
- (35) Shinde, U. A.; Kulkarni, K. R.; Phadke, A. S.; Phadke, A. M.; Mungantiwar, D. V. J.; Saraf, M. N. *Ind. J. Exp. Biol.* **1999**, *37*, 258–261.
- (36) Boman, H. G.; Kaletta, U. *Biochem. Biophys. Acta.* **1957**, *24*, 619–631.
- (37) Ahn, K. H.; Kim, H.; Kim, J. R.; Jeong, S. C.; Kang, T. S.; Shin, H. T.; Lim, G. J. *Bull. Korean Chem. Soc.* **2002**, *23*, 626–628.
- (38) *Molecular Operating Environment (MOE)*, version 2015.10; Chemical Computing Group: Montreal, Canada 2015, <http://www.chemcomp.com>.
- (39) <http://www.rcsb.org>.